

Review

# Vanadium and Melanoma: A Systematic Review

Cristina Amante <sup>1</sup>, Ana Luísa De Sousa-Coelho <sup>2,3,4,\*</sup>  and Manuel Aureliano <sup>5,6,\*</sup> 

<sup>1</sup> Faculdade de Medicina e Ciências Biomédicas (FMCB), Campus de Gambelas, Universidade do Algarve, 8005-139 Faro, Portugal; cristinaamante14@gmail.com

<sup>2</sup> Centre for Biomedical Research (CBMR), Campus of Gambelas, Universidade do Algarve, 8005-139 Faro, Portugal

<sup>3</sup> Algarve Biomedical Center (ABC), Campus de Gambelas, Universidade do Algarve, 8005-139 Faro, Portugal

<sup>4</sup> Escola Superior de Saúde (ESS), Campus de Gambelas, Universidade do Algarve, 8005-139 Faro, Portugal

<sup>5</sup> Faculdade de Ciências e Tecnologia (FCT), Campus de Gambelas, Universidade do Algarve, 8005-139 Faro, Portugal

<sup>6</sup> CCMAR, Campus de Gambelas, Universidade do Algarve, 8005-139 Faro, Portugal

\* Correspondence: alcoelho@ualg.pt (A.L.D.S.-C.); maalves@ualg.pt (M.A.); Tel.: +351-289-900-805 (M.A.)

**Abstract:** The application of metals in biological systems has been a rapidly growing branch of science. Vanadium has been investigated and reported as an anticancer agent. Melanoma is the most aggressive type of skin cancer, the incidence of which has been increasing annually worldwide. It is of paramount importance to identify novel pharmacological agents for melanoma treatment. Herein, a systematic review of publications including “Melanoma and Vanadium” was performed. Nine vanadium articles in several melanoma cells lines such as human A375, human CN-mel and murine B16F10, as well as in vivo studies, are described. Vanadium-based compounds with anticancer activity against melanoma include: (1) oxidovanadium(IV); (2) XMenes; (3) vanadium pentoxide, (4) oxidovanadium(IV) pyridinonate compounds; (5) vanadate; (6) polysaccharides vanadium(IV/V) complexes; (7) mixed-metal binuclear ruthenium(II)–vanadium(IV) complexes; (8) pyridoxal-based oxidovanadium(IV) complexes and (9) functionalized nanoparticles of yttrium vanadate doped with europium. Vanadium compounds and/or vanadium materials show potential anticancer activities that may be used as a useful approach to treat melanoma.

**Keywords:** vanadium; vanadium complexes; vanadium nanoparticles; vanadate; melanoma; cancer



**Citation:** Amante, C.; De Sousa-Coelho, A.L.; Aureliano, M. Vanadium and Melanoma: A Systematic Review. *Metals* **2021**, *11*, 828. <https://doi.org/10.3390/met11050828>

Academic Editor: Guido Crisponi

Received: 28 April 2021

Accepted: 14 May 2021

Published: 18 May 2021

**Publisher's Note:** MDPI stays neutral with regard to jurisdictional claims in published maps and institutional affiliations.



**Copyright:** © 2021 by the authors. Licensee MDPI, Basel, Switzerland. This article is an open access article distributed under the terms and conditions of the Creative Commons Attribution (CC BY) license (<https://creativecommons.org/licenses/by/4.0/>).

## 1. Introduction

The past decades have marked important advances in the traditional view of many roles that metals and their compounds play in biological systems. In fact, metals, inorganic compounds and/or metals-organic frameworks show a diversity of properties that allowed them to present several and distinct biological, environmental and health applications [1–19]. Recent insights into metals applications includes for instance, zinc nanoparticles as feed additives showing more efficiency than zinc salts, increasing growth not only in fish [1] but also in plants [2], besides preventing metal contaminants accumulation [2] and normalizing antioxidant biomarkers [1,2]. Very recently, zinc salts have been referred with a potential use in medicine such for the prevention and treatment of SARS-CoV-2 infection [3,4]. Polyoxotungstates (POTs), such as decatungstate ( $W_{10}O_{32}^{4-}$ ), have shown, by photocatalytic activity, to decompose antibiotics namely sulfasalazine and sulfapyridine with different specificities and rates [5]. Besides green biotechnology applications, it was suggested that some POTs hamper melanoma cancer cells growth through inhibition of aquaporin-3 activity [6], whereas others POTs as well as gold compounds showed specific inhibitory activities for P-type ATPases [7,8].

Removal of metal contaminants, such as for example cadmium, lead, arsenic and uranium from the environmental is still a problem to overcome in the 21st century. Recent studies highlighted the importance of uranyl speciation and the choice of specific chelating

ligands for uranium removal and recovery from wastewater using electrocoagulation, being alizarin and iron electrode the most efficient combination [9]. On the other hand, metals contaminants such as cadmium are known to induce changes in biochemical parameters in brain causing neurological dysfunction that were proposed to be prevented by tomato and/or garlic extracts, in a rat model [10]. In humans, cadmium levels in urine were also found to be associated with an increase of LDL (low density lipoprotein)-cholesterol and a decrease of HDL (high density lipoprotein)-cholesterol, leading to an increased cardiovascular risk [11].

Lithium, the well-known beneficial metal and used in treatment of bipolar disease, has been recently described to partially prevent the increase of  $\text{Na}^+/\text{K}^+$ -ATPase activity induced by sleep deprivation, as observed in rats [12]. In humans, lithium showed to be a  $\text{Na}^+/\text{K}^+$ -ATPase regulator once it was verified that it impeded the decrease of the  $\text{Na}^+/\text{K}^+$ -ATPase activity observed in chorea-acanthocytosis patients [13]. Essential elements such as cobalt could be a good choice in hip prosthesis [14]. However, it was described that cobalt is accumulated and affects differently astrocytes and neurons, inducing cytotoxicity in brain cells [14], whereas functionalized cobalt nanoflakes were described with anticancer activities [15]. Finally, a large number of different vanadium salts and complexes have been investigated and reported to have insulin-enhancing, as well as anticancer properties [16,17]. Regarding vanadium and cancer, the number of articles found are higher for lung ( $n = 80$ ), breast ( $n = 73$ ) and liver ( $n = 70$ ) cancer, medium for colon ( $n = 32$ ), leukemia ( $n = 26$ ) and bone ( $n = 21$ ), whereas lower numbers of studies were found for brain ( $n = 10$ ) and skin ( $n = 8$ ), after a research in the Web of Science.

Although vanadium studies in skin cancer have been scarce, melanoma is the most aggressive type of skin cancer, and its incidence has been increasing annually worldwide at a faster rate compared to any other type of malignant tumor [20,21]. Usually, this pathology is diagnosed early and treated by surgery. On the other hand, its ability to metastasize makes this pathology dangerous [21], which along with patients' relapse driven by the acquisition of therapy resistance [22], makes the search for novel therapeutic targets and options for melanoma treatment a priority [23].

This disease develops from melanocytes, cells found predominantly in the basal layer of the epidermis [20,24,25]. Melanocytes derive embryologically from pluripotent neural crest stem cells, which have high migratory potential [25,26]. This migratory embryonic origin of the melanocytes explains why melanoma is a type of cancer with a high capacity for metastasis [25]. The homeostasis of these melanocytes is controlled by epidermal keratinocytes. These last cells produce a hormone called MSH (melanocyte stimulating hormone), which allows the binding between MC1R (melanocortin 1 receptor) and melanocytes, controlling melanocytes proliferation and preventing the appearance of changes in DNA, through the production of melanin [20]. When skin cells are exposed to excessive ultraviolet (UV) radiation, the formation of malignant melanocytes can be induced through two different mechanisms: direct transformation of normal melanocytes into cancerous melanocytes and the transformation of melanocytes into benign nevi, which subsequently become malignant (Figure 1). Direct targeting of melanocytes normally occurs when mutations in proto-oncogenes and tumor suppressor genes emerge (TP53, NF1, PTEN, etc.). When melanocytes are turned into benign nevi, these can stay that way for decades. However, UV rays can cause the appearance of genetic mutations in the TERT genes (reverse transcriptase of telomerase II) and CDKN2A (cyclin 2A-dependent kinase inhibitor) for example, which lead to malignant transformation of the nevi (Figure 1) [20].

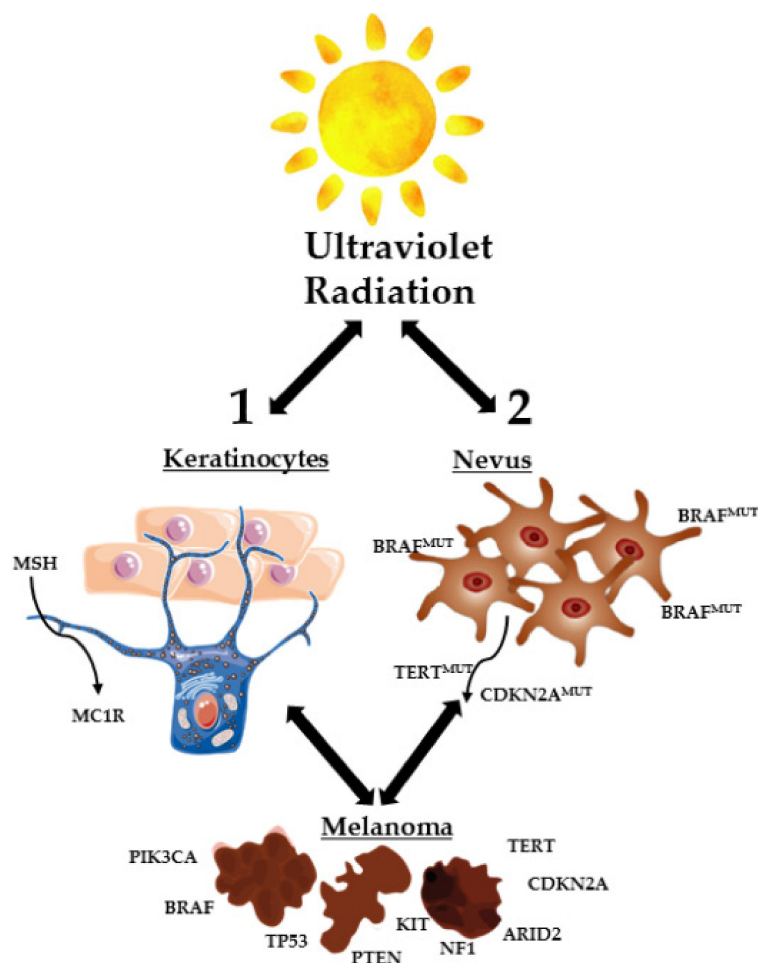


**Figure 1.** Skin cells exposed to excessive UV radiation. Formation of malignant melanocytes by direct transformation of normal melanocytes and/or transformation of melanocytes into benign nevi, which become malignant (adapted from [20]). ARID2, AT-rich interaction domain 2; BRAF, B-Raf proto-oncogene; CDKN2A, cyclin-dependent kinase inhibitor 2A; KIT, KIT proto-oncogene receptor tyrosine kinase; MC1R, melanocortin 1 receptor; MSH, melanocyte stimulating hormone; NF1, neurofibromin 1; PIK3CA, phosphatidylinositol-4,5-bisphosphate 3-kinase catalytic subunit alpha; PTEN, phosphatase and tensin homolog; TERT, telomerase reverse transcriptase; TP53, tumor protein p53.

Herein, a temporal distribution of publications including “Melanoma and Vanadium” was performed. The present systematic review consists of grouping data and their respective analysis, aiming the applications of vanadium compounds in the treatment of melanoma. It is intended to solve the following question: “Are vanadium compounds and/or vanadium materials potential anticancer drugs that can be used to treat melanoma?”

## 2. Methodology

In this systematic review, the following databases were chosen: Clinical Trials, Cochrane Library, Pubmed/Medline, Scielo and Web of Science. Search terms used were: “Melanoma AND vanadium” and “Melanoma AND vanadate”. The literature search was carried out between the 10 March 2021 and the 31 March 2021.

Inclusion and exclusion criteria were defined to select the articles with more relevance to this study (Figure 2, steps 5 and 6, respectively).

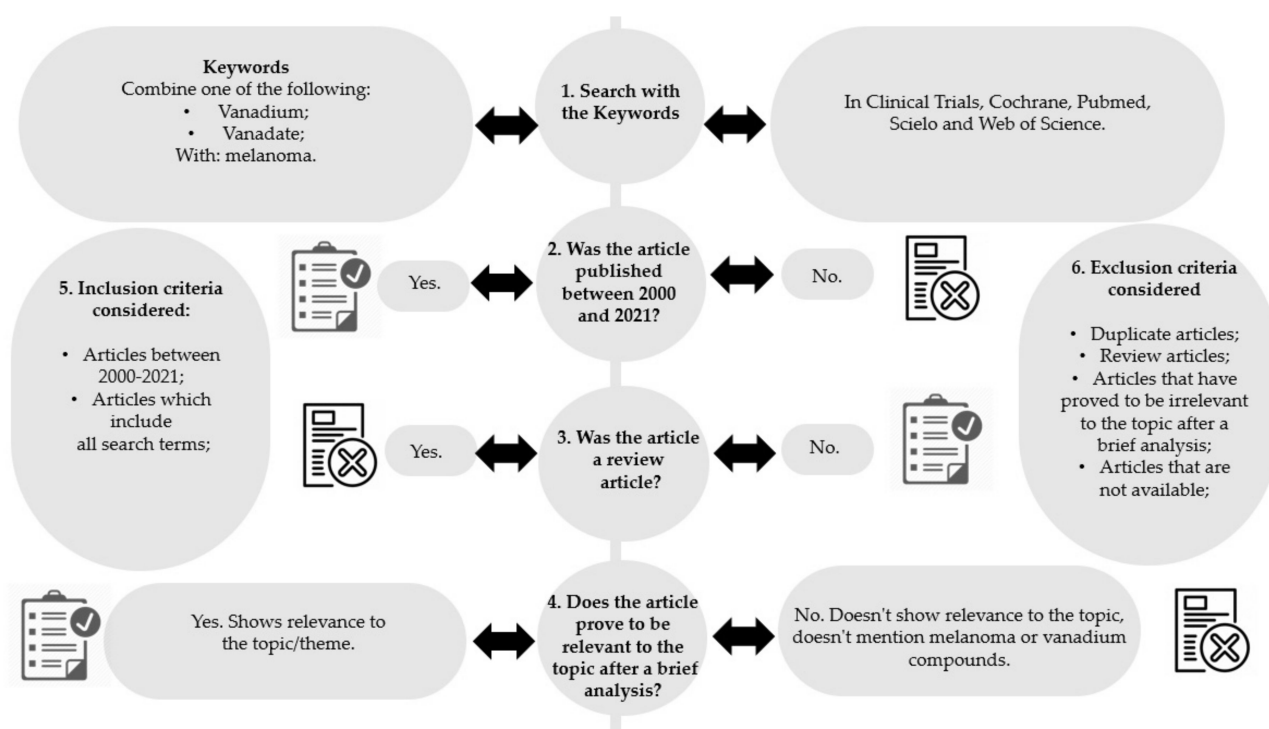


**Figure 2.** Methodology diagram of the articles' selection process.

After the initial research (Figure 2, step 1), articles which were relevant to the topic were selected by at least two independent researchers, by applying the following steps:

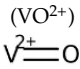
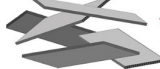
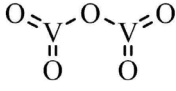
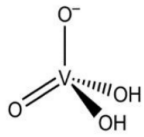
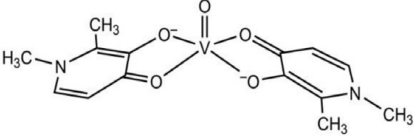
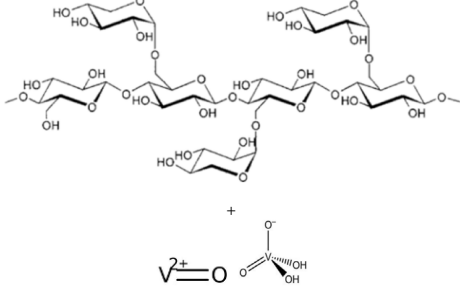
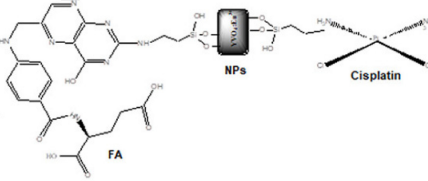
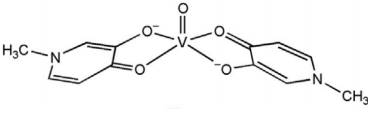
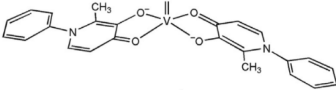
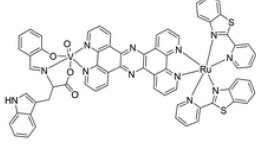
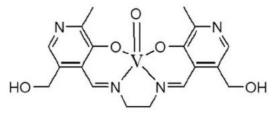
1. Removal of articles not published between 2000 and 2021 (Figure 2, step 2);
2. Removal of review articles (Figure 2, step 3);
3. Evaluation of titles/abstracts and obtaining all articles potentially relevant;
4. Confirmation of the relevance or irrelevance of the articles obtained, checking for factors that would imply inclusion/exclusion, through the reading of the full articles (Figure 2, step 4);
5. Organization of selected studies in a reference management program.

After selecting the articles with relevance to the topic, the data were grouped and treated. Subsequently, the results of the various investigations were studied, and the methods, doses and treatment durations, types of samples and models used, were analyzed. The summary of the methodology used is outlined in Figure 2. From the twenty-one studies found, twelve were eliminated, of which: nine articles for not being dated between 2000 and 2021; two articles because they were a review; and one article for being irrelevant to the topic. Finally, nine articles were considered for this review.

### 3. Types of Vanadium Based-Compounds Used in Studies against Melanoma

Among the eleven vanadium, vanadium complexes and/or materials found in the nine articles selected, eight are vanadium (IV), and/or vanadium (V) compounds, two represents vanadium nanoparticles (NPs) (compounds 3 and 7) and one is an emergent material from the family of early transition metal carbides/nitrides referred to as MXenes (compound 2) (Table 1). Regarding the eight vanadium(IV/V) solutions, seven are complexes of oxidovanadium (IV) and/or salts of oxidovanadium (compounds 1, 5, 6, 8, 9, 10 and 11) and one is the monomeric vanadate species itself (compound 4). The structure of these vanadium compounds and/or vanadium materials [27–35] are represented in Table 1. It should be noted that compound 6 can be formed with both vanadium oxidation states IV (oxidovanadium(IV)) and V (vanadate) being compounds 4 and 5 described in two articles [30,31], while compounds 5, 8 and 9 were referred in the same article [31] (Table 1).

**Table 1.** Representation of the structures of vanadium compounds and/or vanadium materials included in the review.

Vanadium Compound/Material	Structure	Year (Ref)
VOSO <sub>4</sub> Vanadyl sulfate (Abbreviated VO) 1	(VO <sup>2+</sup> ) 	2021 [27]
V <sub>2</sub> CT <sub>z</sub> -Ox <sub>24</sub> / V <sub>2</sub> CT <sub>z</sub> -Ox <sub>48</sub> (V2CTz) Vanadium carbides (MXenes) 2	 s-V <sub>2</sub> CT <sub>z</sub>	2020 [28]
V <sub>2</sub> O <sub>5</sub> Vanadium pentoxide (VP) 3		2020 [29]
H <sub>2</sub> VO <sub>4</sub> <sup>−</sup> monomeric vanadate (VN) 4		2019 [30], 2017 [31]
V <sup>IV</sup> O(dhp) <sub>2</sub> (VS2) dhp: 1,2-dimethyl-3-hydroxy-4(1H)-pyridinonate 5		2019 [30], 2017 [31]
Xyloglucan oxovanadium (IV/V) (XGCVO) 6		2018 [32]
Y <sup>III</sup> V <sup>V</sup> O <sub>4</sub> : Eu <sup>III</sup> (YVEu NPs) Europium(III)-doped yttrium vanadate nanoparticles 7		2018 [33]
[V <sup>IV</sup> O(mpp) <sub>2</sub> ] (VS3) mpp: 1-methyl-3-hydroxy-4(1H) pyridinonate 8		2017 [31]
[V <sup>IV</sup> O(ppp) <sub>2</sub> ] (VS4) ppp: 1-phenyl-2-methyl-3-hydroxy-4(1H)-pyridinonate 9		2017 [31]
[Ru-(pbt) <sub>2</sub> (tpphz)VO(sal-L-tryp)]Cl <sub>2</sub> (RuVO) pbt = 2-(2'-pyridyl)benzothiazole tpphz = tetrapyrido [3,2-a:2',3'-c:3'',2''-h:2''',3'''-j]phenazine sal-L-tryp = N-salicylidene-L-tryptophan 10		2013 [34]
N,N'-ethylenebis (pyridoxylideneiminat) vanadium (IV) complex (Pyr <sub>2</sub> enVO) 11		2013 [35]



## 4. Vanadium Species, Complexes and/or Materials Effects in Melanoma Cells

### 4.1. Cell Viability Effects

B16F10 cells (murine skin melanoma) were treated with several concentrations of vanadyl sulfate ( $\text{VOSO}_4$ ) (compound 1), treated with or without recombinant Newcastle disease virus (NDV). NDV, is an oncolytic agent that has been study in pre-clinical cancer models and human clinical trials [36]. After 48 h, the cellular metabolic ability was measured using the resazurin assay. Vanadyl plus NDV reduced the metabolic activity of B16F10 cells, showing that cell viability decreased between 45% and 90%, 90% at the highest concentration used of  $\text{VOSO}_4$  (200  $\mu\text{M}$ ). The combination between vanadyl (oxidovanadium(IV)) and the oncolytic agent NDV showed further decrease in cell viability than either  $\text{VOSO}_4$  or NDV alone, being dose-dependent. While using  $\text{VOSO}_4$  alone reduced over 50% of metabolic activity only from 100  $\mu\text{M}$  and above, the combination with NDV showed a similar inhibitory effect at the lowest dose of  $\text{VOSO}_4$  tested (0.78  $\mu\text{M}$ ) [27].

The effects of  $\text{V}_2\text{CT}_z\text{-ox}_{24}/\text{V}_2\text{CT}_z\text{-ox}_{48}$  (compound 2) were studied in A375 cells (human malignant melanoma) and in HaCaT cells (immortalized keratinocytes). Cells were treated with several concentrations of the two MXenes and an MTT (3-(4,5-dimethylthiazol-2-yl)-2,5-diphenyltetrazolium bromide) assay was done to measure the metabolic activity of the cells, as a measure of cellular viability. Comparing both MXenes, the results showed that  $\text{V}_2\text{CT}_z\text{-ox}_{48}$  provided a higher decrease in cell viability: in A375 cells, cells viability decreased between 28–65%; in HaCaT cells, cells viability decreased between 25% and 60%.  $\text{V}_2\text{CT}_z\text{-ox}_{24}$  showed a decrease between 15% and 55% in A375 cells and between 2% and 30% in HaCaT cells. The highest decrease in cell viability was detected at the highest concentrations used (200  $\mu\text{g}/\text{mL}$ ), in both cell lines. While a decrease of 50% of cellular viability was observed with 25–50  $\mu\text{g}/\text{mL}$  of  $\text{V}_2\text{CT}_z\text{-ox}_{24}$  only in A375 melanoma cells, a comparable inhibitory effect was achieved with 1–5  $\mu\text{g}/\text{mL}$  of  $\text{V}_2\text{CT}_z\text{-ox}_{48}$ , in both cell lines [28].

B16F10 cells were treated with several concentrations of vanadium pentoxide ( $\text{V}_2\text{O}_5$ ) (compound 3) during 24 h. The MTT assay showed that the viability of the cells, treated with increasing doses of  $\text{V}_2\text{O}_5$ , decreased up to 70% with the highest concentration used (50  $\mu\text{g}/\text{mL}$ ), showing dose-dependent inhibition levels between 15% and 70%. A decrease of 50% of cellular viability was observed upon treatment with 10  $\mu\text{g}/\text{mL}$  in melanoma cells [29].

Cytotoxic activity for compounds 4, 5, 8 and 9 (VN, VS2, VS3, and VS4, respectively) was evaluated by MTT assay in A375 and CN-mel (human noncutaneous metastatic melanoma [37]) cells. Both cell lines were treated for 72 h at three different concentrations (1, 10 and 100  $\mu\text{M}$ ) of each vanadium compound [30,31]. At the lowest concentration, cells did not show accentuated signs of decreased cell viability. On the other hand, at 10 and 100  $\mu\text{M}$ , A375 cells underwent a marked decrease in cell viability, presenting viability values never greater than 2% for all compounds, regardless of the concentration tested. CN-mel showed a less accentuated decrease, having viability values between 52% and 59% at 10  $\mu\text{M}$  but even so, at the highest concentration (100  $\mu\text{M}$ ), there was a more pronounced decrease viability, with viability values between 1.5% and 13%. In these conditions,  $\text{IC}_{50}$  values between 2.4 and 4.7  $\mu\text{M}$  were found for A375 cells and between 6.5 and 14  $\mu\text{M}$  for CN-mel cancer cells. The relative order of potency for human noncutaneous metastatic melanoma was found to be compound 4 > 8 > 5 > 9 whereas for human malignant melanoma, the potency was different namely compound 8 > 5 > 9 > 4.

B16F10 cells were treated with several concentrations of compound 6, XGC:VO, which was cytotoxic in a concentration-dependent fashion. After 24 h of incubation, XGC:VO treatment decreased cells viability by 23% and 50% at 2.5  $\mu\text{g}/\text{mL}$  and 300  $\mu\text{g}/\text{mL}$ , respectively, though similar to what was observed with the polysaccharide XGC alone [32].

When treated with compound 11,  $\text{Pyr}_2\text{enVO}$ , in the only concentration used (50  $\mu\text{M}$ ) and incubated for 72 h, the results showed 93% of cell death in A375 cells. Under these conditions,  $\text{IC}_{50}$  values ( $\mu\text{M}$ ) of 61.5 (24 h), 13.0 (48 h) and 6.0 (72 h) were found. Similarly, when treated with  $\text{Pyr}_2\text{en}$  solo (50  $\mu\text{M}$ ), cell mortality in A375 cells was around 18% [35].

#### 4.2. Cell Morphology and Apoptosis Effects

To find out if apoptosis or necrosis occurs when A375 melanoma cells are incubated with compound **2**  $V_2CT_z-ox_{24}/V_2CT_z-ox_{48}$  for 24 h, a cytometric analysis using Annexin V-FITC and propidium iodide (PI) was performed. When performed in HaCaT cells, the results showed that the population of apoptotic cells was negligible, showing that the MXenes are biocompatible with keratinocytes (over 70% survivability). A375 cells exposed to the highest concentrations of s- $V_2CT_z-ox_{48}$  showed the highest percentage of necrotic cells [28].

B16F10 cells were incubated with compound **3** ( $V_2O_5$ ) and with SU-5416 (semaxanib) for 18 h [29]. SU-5416 was used as a positive control, since this substance is an inhibitor of angiogenesis and leads to suppression of tumors through the induction of apoptosis [35,38]. Flow cytometry assay showed that cells treated with  $V_2O_5$  or with SU-5416 showed an increase in the apoptotic region in the single tested concentration (10  $\mu\text{g}/\text{mL}$ ), in relation to untreated cells. A TUNEL assay was also performed in the same conditions and the results exhibited TUNEL positivity with  $V_2O_5$  (10  $\mu\text{g}/\text{mL}$ ) and SU-5416 (20 nM) for 18 h, indicating DNA damage.

Apoptosis evaluation tests were performed on cells treated with compounds **4** and **5** (VN and VS2, respectively) in two different articles [30,31], having counted the live, apoptotic and necrotic cells. In Pisano, et al. [30] untreated and treated cells were also treated with NAC (N-acetylcysteine), a ROS inhibitory compound [39], as control. The Annexin V apoptosis assays suggested that treatments with the longer duration (48 h) and higher doses cause a larger apoptotic effect in A375 cells. VN increased apoptotic population up to 48%, while VS2 increased apoptotic population up to 52%, at the highest concentration used (20  $\mu\text{g}/\text{mL}$ ) in 48 h assays. In Rozzo, et al. [31], the Annexin V apoptosis assays suggested that treatments with the longer duration (72 h) and higher doses cause larger apoptotic effects in A375 cells, as well. VN increased apoptotic population up to 70%, while VS2 increased apoptotic population up to 67%, at the highest concentration used (20  $\mu\text{g}/\text{mL}$ ) in 72 h assays.

Apoptotic analysis using flow cytometry was carried out to study the apoptotic effects of compound **6** (XGC:VO) and XGC alone, in B16F10 cells [32]. Cells were studied after 24 h treatments. The number of apoptotic cells increased 50% after treatment with XGC:VO, at the highest concentration used (200  $\mu\text{g}/\text{mL}$ ). In additional concentrations (5 and 25  $\mu\text{g}/\text{mL}$ ) and in cells treated with XGC (in all concentrations used), the appearance of apoptotic cells was considered by the authors to be mild.

Finally, cell morphology changes were described for compound **10** [34]. This, in the tests with the compound **10**,  $\text{Ru}-(\text{pbt})_2(\text{tpphz})\text{VO}(\text{salt-L-trypt})$ , malignant cells of human amelanotic melanoma were used. The studies were carried out at concentrations of 5 and 20  $\mu\text{M}$ , differing in the absence/presence of light. Both conditions were treated in the same way. Briefly, after 24 h of treatment, cells were incubated for 30 min in light or in the dark, and after 3 h the photos were taken using the microscope. The results indicated that death occurred in treated cells in the presence of light at the highest concentration of compound **10** (20  $\mu\text{M}$ ), although there are also some effects at the lowest concentration (5  $\mu\text{M}$ ). Table 2 includes the effects referred above for the cellular viability, morphology and apoptosis effects of the vanadium compounds, as well as the effects described in the following sections namely: cell cycle effects, ROS production, mitochondrial effects, proteins expression studies and additionally in vivo anticancer activities such as tumor regression and survival rates.

**Table 2.** Vanadium compounds and materials effects in human melanoma cells lines, namely A375 (human malignant melanoma), CN-mel (human metastatic melanoma), amelanotic melanoma and B16F10 (Mus musculus skin melanoma) namely in: Cell viability, cell morphology and apoptosis effects, cell cycle effects, ROS production, mitochondrial effects and protein expressions. Mice in vivo anticancer studies are also included.

Compound	Cell Viability	Cell Morphology and Apoptosis Effects	Cell Cycle Effects	ROS Production	Mitochondrial Effects	Protein Expressions Studies	In Vivo Anticancer Activity
VO 1	<b>B16F10 cells</b> 200 $\mu$ M produces 90% inhibition, after 48 h						<b>Mice</b> Tumor regression upon VOSO <sub>4</sub> (40 mg/kg), 96 h
V <sub>2</sub> CTz 2	<b>A375 cells</b> 50% inhibition for 1–5 $\mu$ g/mL V <sub>2</sub> CTz-ox <sub>48</sub> and for 25–50 $\mu$ g/mL V <sub>2</sub> CTz-ox <sub>24</sub>	<b>A375 cells</b> The population of apoptotic cells was negligible, for 24 h	<b>A375 cells</b> Cellular cycle arrest in the G <sub>0</sub> /G <sub>1</sub> phase, triggering apoptosis	<b>A375 cells</b> V <sub>2</sub> CTz-ox <sub>24</sub> increased ROS to 225%, (100 $\mu$ g/mL) V <sub>2</sub> CTz-ox <sub>48</sub> increased ROS to 140% (100 $\mu$ g/mL)	<b>A375 cells</b> s-V <sub>2</sub> CTz-ox <sub>48</sub> , slight increase mitochondrial membrane potential ( $\Delta\Psi$ m)		
VP 3	<b>B16F10 cells</b> 50% inhibition for 10 $\mu$ g/mL	<b>B16F10 cells</b> Increase of apoptosis (10 $\mu$ g/mL), for 18 h DNA damage (10 $\mu$ g/mL), for 18 h		<b>B16F10 cells</b> Anion superoxide formation (10 $\mu$ g/mL)		<b>B16F10 cells</b> Upregulation of p53 downregulation of anti-apoptotic survivin (10, 20 $\mu$ g/mL)	<b>Mice</b> The survival rate increased up to 47 days, (10 mg/kg) No changes: body weight; in feed intake. No toxicity in vital organs
VN 4	<b>A375 cells</b> IC <sub>50</sub> = 4.7 $\mu$ M, 72 h  CN-mel IC <sub>50</sub> = 6.5 $\mu$ M, 72 h	<b>A375 cells</b> Pisano, et al. Increased apoptotic population to 48%, (20 $\mu$ g/mL), 48 h. Rozzo, et al. Increased apoptotic population to 70%, (20 $\mu$ g/mL), 72 h	<b>A375 cells</b> Cells did not go through the G <sub>2</sub> /M phase, dying through apoptosis	<b>A375 cells</b> ROS increased to 80% (20 $\mu$ g/mL), 48 h.		<b>A375 cells</b> ph-ERK, ph-Rb and ph-Cdc25c levels decreased to 20% (20 $\mu$ M), 24 h, p21Cip1 rised up to 10-14 times (20 $\mu$ M)	
VS2 5	<b>A375 cells</b> IC <sub>50</sub> = 2.6 $\mu$ M, 72 h  CN-mel IC <sub>50</sub> = 12.4 $\mu$ M, 72 h	<b>A375 cells</b> Pisano, et al. Increased apoptotic population up to 52%, at the highest concentration used (20 $\mu$ g/mL) in 48 h assays. Rozzo, et al. Increased apoptotic population up to 67%, at the highest concentration used (20 $\mu$ g/mL) in 72 h assays	<b>A375 cells</b> Cell cycle arrested in G <sub>0</sub> /G <sub>1</sub> phase, showing not to be able to enter the S phase.	<b>A375 cells</b> ROS levels increasing up to 80% as well, at the highest duration (48 h) and dose (20 $\mu$ g/mL).		Pisano, et al. <b>A375 cells</b> ph-ERK, ph-Rb and ph-Cdc25c levels decreased to 20% (20 $\mu$ M), p21Cip1 levels increased up to 18 times (20 $\mu$ M) Rozzo, et al. Increasing of the cleaved PARP band (85 kD)	



Table 2. Cont.

Compound	Cell Viability	Cell Morphology and Apoptosis Effects	Cell Cycle Effects	ROS Production	Mitochondrial Effects	Protein Expressions Studies	In Vivo Anticancer Activity
XGCVO 6	B16F10 cells 50% inhibition at 300 µg/mL	B16F10 cells 50% increase of apoptosis (200 µg/mL)	B16F10 cells Cell cycle has not changed		B16F10 cells Mitochondrial respiration decreased to 43% (5 µg/mL) 34% pyruvate decrease No effects lactate production		
YVEu NPs 7							Mice Tumor regression upon Y <sup>III</sup> V <sup>V</sup> O <sub>4</sub> :Eu <sup>III</sup> ; CPTES:FA: CDDP (15 mg/kg), 5 days; CDDP toxicity reduced
VS3 8	A375 cells IC <sub>50</sub> = 2.4 µM, 72 h CN-mel IC <sub>50</sub> = 10.4 µM, 72 h						
VS4 9	A375 cells IC <sub>50</sub> = 4.2 µM, 72 h CN-mel IC <sub>50</sub> = 14.0 µM, 72 h						
RuVO 10		Amelanotic melanoma In the absence of light, changes in cell morphology (20 µM). In the presence of light, apoptosis observed, 20 µM.					Mice The survival rate was 100%. Tumor weight reduction. Proliferative activity reduction
Pyr <sub>2</sub> enVO 11	A375 cells IC <sub>50</sub> = 61.5 (24 h) IC <sub>50</sub> = 13.0 (48 h) IC <sub>50</sub> = 6.0 (72 h)		A375 cells Increase of G0/G1 cells to 60% (100 µM), 72 h	A375 cells ROS increased to 23% (100 µM), 24 h	A375 cells Percentage of cells with loss of ΔΨ <sub>m</sub> increased up to 35% (100 µM), 48 h, and 73%, after 72 h		

### 4.3. Cell Cycle Effects

To assess the effects on the cell cycle of cells treated with compound **2** (V<sub>2</sub>CTz-ox24 and V<sub>2</sub>CTz-ox48), a PI staining was performed. HaCaT cells suffered a small increase of G<sub>0</sub>/G<sub>1</sub> phase in the maximum duration treatment (48 h), leading to an increased cell size. A375 suffered cellular cycle arrest in the G<sub>0</sub>/G<sub>1</sub> phase, triggering apoptosis. A small increase in the number of melanoma cells in G<sub>2</sub>/M phase was observed [28].

Tests were carried out on A375 cells, with compounds **4** and **5** (VN and VS2, respectively), to evaluate the effects on cell cycle progression through PI cell staining [31]. Cells treated with two different concentrations of VN and VS2 (10 and 20 µg/mL), for 24 h, 48 h and 72 h, were studied. Cells treated with compound **4** (VN) for 48 h and 72 h did not survive for such periods, so it was not possible to evaluate the cell cycle progression. When treated with compound **4**, VN, for 24 h, A375 cells did not go through the G<sub>2</sub>/M phase, dying through apoptosis. In cells treated with compound **5**, VS2, the cell cycle arrested in G<sub>0</sub>/G<sub>1</sub> phase, showing not to be able to enter the S phase [31].

After A375 cells were treated with several concentrations of compound **11** Pyr<sub>2</sub>enV(IV), they were labeled with PI and subsequently analyzed by flow cytometry to measure the percentage of apoptotic nuclei sub-G<sub>0</sub>/G<sub>1</sub>. Cells treated with the highest concentration used (100 µM) showed a percentage of Sub G<sub>0</sub>/G<sub>1</sub> cells over 60%, in 72 h treatments. The results showed to be dose and duration dependents [35].

### 4.4. Effects on ROS Production

The level of intracellular reactive oxygen species (ROS) was measured using non-specific fluorescent dye (DCF-DA), when HaCaT and A375 cells were incubated with different concentrations of compound **2** (V<sub>2</sub>CTz-ox24 and V<sub>2</sub>CTz-ox48) for 48 h. V<sub>2</sub>CTz-ox24 increased ROS levels up to 225% in A375 cells (100 µg/mL) and ~210% in HaCaT cells (50 µg/mL). ROS levels caused by incubation with V<sub>2</sub>CTz-ox48 showed lower ROS levels in A375 cells compared to the other MXene, increased only up to 140% at the highest concentration (100 µg/mL). In HaCaT cells, ROS levels increased up to 245%, at 50 µg/mL with V<sub>2</sub>CTz-ox48, being the highest value obtained (Table 2) [28].

B16F10 cells were treated with DHE (dihydroethidium) reagent after compound **3** V<sub>2</sub>O<sub>5</sub> nanoparticles (10 µg/mL) and SU-5416 (20 nM) exposure to determine the intracellular anion superoxide production. Cells treated with V<sub>2</sub>O<sub>5</sub> or SU-5416, displayed red fluorescence indicating the formation of intracellular ROS, suggesting that the formation of superoxide could be the plausible mechanism for the anticancer activity of vanadium pentoxide [29].

A375 cells were treated with compounds **4** and **5**, VN and VS2 and the percentage of ROS that appeared after treatments was measured through flow cytometry assay [30]. Percentages of ROS were checked in absence/presence of NAC (N-acetylcysteine). The increase of ROS with VN showed to be dependent on the treatment duration, showing no differences between the two doses used (10 and 20 µg/mL). ROS formation increased up to ~78% at the highest duration (48 h) and dose (20 µg/mL) used. VS2 showed to be dependent on the duration and dose of the treatment, showing ROS formation increasing up to ~78% as well, at the highest duration (48 h) and dose (20 µg/mL) [30].

In the studies of compound **11** Pyr<sub>2</sub>enVO assay, A375 cells were also treated with Pyr<sub>2</sub>en alone and NAC was also used to inhibit the generation of ROS [35]. The results, obtained through flow cytometry, showed that the percentage of ROS formation did not exceed 23% (with or without NAC), reaching this value in cells treated for 24 h with the single tested concentration (100 µM) of Pyr<sub>2</sub>enVO. The increase of ROS was dependent of the duration of treatment. Cells treated with Pyr<sub>2</sub>en alone did not show ROS generation [35].

### 4.5. Effects on Mitochondria Function

Mitochondrial activity after the exposure of A375 and HaCaT cells to compound **2** s-V<sub>2</sub>CTz-ox24 and s-V<sub>2</sub>CTz-ox48 at several concentrations was determined by monitoring the level of mitochondrial membrane potential ( $\Delta\Psi_m$ ) using the JC-10 dye [28]. HaCaT

cells suffered a slight decrease in the  $\Delta\Psi_m$ , in the presence of both MXenes. On the other hand, A375 cells exposed to s-V<sub>2</sub>CTz-ox48 suffered a slight increase of the  $\Delta\Psi_m$ .

The effects on the respiration of B16F10 cells treated with compound 6 XGC:VO (5 and 25 µg/mL) for 24 h were studied by high-resolution respirometry in an Oxygraph-2k [32]. The results showed an inhibition of cellular respiration. Thus, in the basal state, cells respiration decreased up to 43% and 54% in treatments with 5 and 25 µg/mL, respectively. On the uncoupled state, XGC:VO inhibited the cells respiration up to 60% in treatments with 5 and 25 µg/mL. The effects of XGC:VO (5 and 25 µg/mL for 24 h) in the production of lactate and pyruvate by B16F10 cells were also studied. The treatment with the complex resulted in a decrease of about 34% and 22.5% in the production of pyruvate, for concentrations 5 and 25 µg/mL, respectively. Still, XGC:VO did not alter the production of lactate (Table 2).

Finally, measurement of mitochondrial membrane potential ( $\Delta\Psi_m$ ) was done by flow cytometry (FL-2 channel) in A375 cells treated with 100 µM of compound 11 Pyr<sub>2</sub>enVO or vehicle (Pyr<sub>2</sub>en) for 24, 48 and 72 h. The results showed that the percentage of cells with a potential loss was 34.65% after 48 h and rose to 73.24% after 72 h [35].

#### 4.6. Protein Expressions Effects

To begin dissecting cellular mechanisms of action, B16F10 cells treated with compound 3 V<sub>2</sub>O<sub>5</sub> NPs (10–20 µg/mL) were studied through Western blot, checking the differential apoptotic proteins expression. The results demonstrated upregulation of p53 and downregulation of anti-apoptotic protein survivin, corroborating with the apoptosis and cell cycle analysis [29].

In Pisano, et al. [30], A375 cells were treated with the compounds 4 and 5, VN and VS2, at two different concentrations (10 and 20 µM), for several time intervals (3, 6, 16 and 24 h). To study the levels of expression and/or activation of some key proteins that regulate the initiation and progression of cell cycle, Western blot experiments were carried out using specific antibodies for several proteins. A375 cells, after treatments with VN and VS2, suffered a gradual decrease up to 20% in the levels of ERK phosphorylation (P-ERK). On the other hand, the levels of total ERK protein expression remained unchanged, after both treatments. Levels of P-Rb suffered a gradual decrease, reaching levels of 0% and 10%, respectively after 16 h of treatments with VN (20 µM) and after 24 h of treatments with VS2 (10 µM). The expression of the CDK inhibitor p21Cip1 increased during the first hours (3 and 6 h) of treatment with the two compounds. p21Cip1 increased up to 10–14 times in compound 4, VN-treated cells, and up to 18 times in VS2 treated cells. When P-Cdc25c was studied, the results showed a 20% and 10% decrease in 10 and 20 µM VN/VS2 treated cells, respectively. After treatments with compound 5, VS2 (10 and 20 µM), A375 cells were subjected to a Western blot in Rozzo, et al. [31]. The assay showed an increasing of the cleaved PARP band (85 kD) and decreasing of the whole PARP band (116 kD), dose-dependent, confirming apoptosis (Table 2).

#### 4.7. Anticancer Effects In Vivo

C57BL/6 mice were implanted with B16F10 tumor cells intradermally and when the tumors reached 5 mm in diameter, the treatments were initiated. The groups of animals were either injected intratumorally with phosphate-buffered saline (PBS), compound 1 VOSO<sub>4</sub> (20 mg/kg or 40 mg/kg), Newcastle disease virus (NDV) solo, or a combination of VOSO<sub>4</sub> plus NDV, every 48 h for a total of 3 treatments. The treatments ended when tumors reached 15 mm in a single direction. The results showed that there was a fast tumor regression in mice treated with VOSO<sub>4</sub> (40 mg/kg) plus NDV, after only 96 h. On the other hand, when mice were treated with a lower dose of VOSO<sub>4</sub> (20 mg/kg) plus NDV, 50% of the mice were cured of their disease [27]. After the animals were cured, the authors studied the hypothesis that treatment induced a tumor-specific memory. Mice were once again injected with B16F10 tumor cell, intravenously and subcutaneously, without any

treatments there was no increase in survival rate when compared to controls, disproving the proposed hypothesis [27].

Still regarding compound 1, the effects on the tumor microenvironment (TME) and in tumor-draining lymph nodes (TdLNs) were studied. When tumors reached 8 mm in any one direction, the therapy was administered and after 36 h tumors were harvested from the mice. The therapy consisted in a single intratumoral treatment with PBS, vanadyl sulfate (40 mg/kg), NDV or in a combination of vanadyl sulfate plus NDV. Several leukocyte subsets were quantified by flow cytometry and the results showed that the relative number of IFN- $\gamma$  (producing NK cells) in the TME and in TdLNs increased in the combination treatment, indicating that this therapy potentiates the innate immune response [27].

It was also studied the cytotoxic potential of NK cells and the presence of M2 macrophages in tumors harvest from mice administered with a single intratumoral injection of PBS, vanadyl sulfate (40 mg/kg), NDV ( $5.0 \times 10^7$  PFU), or vanadyl sulfate 4 h prior to NDV, after 24 h. It was performed tumor-infiltrating lymphocyte (TIL) analysis using a specific antibody panel for this concrete study. The results showed that vanadyl sulfate plus NDV provoked the highest percentage of NK cells producing granzyme B, a cytotoxic serine protease found in the granules of NK cells. The results also showed that the number of M2 macrophages, identified through the presence of CD206, was reduced in treatments with vanadyl sulfate plus NDV. The therapy with vanadyl sulfate plus NDV enhanced the cytolytic potential of NK cells, while simultaneously decreased the immunosuppressive nature of the tumor microenvironment [27]. To investigate how this combination therapy alters the cytokine profile in the tumor microenvironment, tumor's cytokines were quantified in tumors harvested 36 h after treatments with PBS, vanadyl sulfate (40 mg/kg), NDV ( $5.0 \times 10^7$  PFU) or of vanadyl sulfate in combination with NDV, using a flow cytometry. There was an increase in the percentages of IFN- $\beta$ , GM-CSF, MCP-1 (CCL2) and IL-6, while there was a decrease in percentages of IL-1 $\beta$ . Also, NDV or vanadyl sulfate plus NDV both increased the percentages of CXCL-10 and CCL5. The combination therapy showed changes in the cytokine profile in the TME.

To study the efficacy of compound 2  $V_2O_5$  in vivo, female C57BL/6J mice were injected subcutaneously in the lower right abdomen with B16F10 cells [29]. Later, a study was carried out to verify the animals' ability to survive. Thus, four groups of three mice were treated with different concentrations of vanadium pentoxide (0, 1, 5 and 10 mg/kg). Doses were administered intra-peritoneally when tumors reached 50–10 mm<sup>3</sup>, every 7 days. It was found that after treatments, the animals' survival rate increased, in comparison to untreated mice, at the highest dose used. It was also performed an assay to study the sub chronic toxicity of  $V_2O_5$ . Three groups of 5 mice were treated with 0, 10 mg/kg of  $V_2O_5$  NPs and 20 mg/kg of  $V_2O_5$  NPs, injected intra-peritoneally for 7 consecutive doses for a period of 28 days. The results showed that  $V_2O_5$  NPs did not bring changes in body weight or in feed intake. After sacrifice of the mice that underwent the study of sub chronic toxicity, several analyses to assess the effects caused by the administration of  $V_2O_5$ , namely a histopathological analysis, were performed. Globally, the mice did not show changes in the organs, and only some changes appeared, such as fatty degeneration in the liver tissues (when treated with a dose of 20 mg/kg) and mild peri-biliary fibrosis (when treated with a dose of 10 mg/kg).

Finally, the antitumor efficiency of chemotherapy with cisplatin (CDDP) alone and incorporated into the compound 7  $Y^{III}V^VO_4:Eu^{III}$  NPs in vivo, was evaluated [33]. Male C57BL/6 mice were injected subcutaneously into the right dorsolateral region with viable B16F10 cells. When the tumor had reached approximately 100 mm<sup>3</sup> (18 days after cell implantation), five groups of five mice were treated with different compounds, such as 15 mg/kg of  $Y^{III}V^VO_4:Eu^{III}$ , 15 mg/kg of  $Y^{III}V^VO_4:Eu^{III}$ : CPTES (3-chloropropyltrimethoxy silane), 15 mg/kg of  $Y^{III}V^VO_4:Eu^{III}$ :CPTES:CDDP, 15 mg/kg of  $Y^{III}V^VO_4:Eu^{III}$ : CPTES:FA: CDDP and 5 mg/kg of CDDP, once a day and for 5 consecutive days. The survival rate of the mice studied was 70% in the CDDP group and 100% in all other groups. Furthermore, the group treated with CDDP solo, exhibited weight loss and liver weight decreased

about 44%. It was observed that there was tumor weight reduction when treated with  $Y^{III}V^VO_4:Eu^{III}:CPTES:CDDP$ ,  $Y^{III}V^VO_4:Eu^{III}:CPTES:FA:CDDP$  and  $CDDP$ , but not when treated with  $Y^{III}V^VO_4:Eu^{III}$  and  $Y^{III}V^VO_4:Eu^{III}:CPTES$ .

After the sacrifice of the mice, histopathological analysis showed a reduction in proliferative activity in mice treated with  $Y^{III}V^VO_4:Eu^{III}:CPTES:CDDP$ ,  $Y^{III}V^VO_4:Eu^{III}:CPTES:FA:CDDP$  and  $CDDP$ , but not when treated with  $Y^{III}V^VO_4:Eu^{III}$  and  $Y^{III}V^VO_4:Eu^{III}:CPTES$ . It was also performed a micronucleus assay through Trypan blue exclusion, which assesses the frequency of micronuclei (genotoxic damage indicators) and this showed that there is a greater micronuclei formation in animals treated with  $Y^{III}V^VO_4:Eu^{III}:CPTES:CDDP$  only. Biochemical analysis suggested that treatment with  $CDDP$  causes nephrotoxicity [33]. The effects described above are briefly summarized in Table 2.

## 5. Discussion

The several applications of the diversity of vanadium species, compounds, complexes and polyoxovanadates, including anticancer activities, drew attention of scientists in recent decades due to its effects against various types of diseases [16,17,27–35,40–45]. With this review, we intend to make a comprehensive collection of updated information about the potential use of vanadium compounds in the treatment of melanoma, from studies already carried out, to facilitate and optimize future research.

### 5.1. Vanadyl

The use of the combination of compound 1, vanadyl sulfate, with the oncolytic virus NDV decreased the metabolic activity of B16F10 cells [27]. The authors associated this antiproliferative action with the fact that  $VOSO_4$  made the cells more permissive to NDV-induced apoptosis, since vanadium compounds have been shown to activate several transcription factors, such as NF- $\kappa$ B [46]. Besides vanadyl (oxidovanadium(IV)), vanadate (vanadium(V)) also increased NDV-mediated cell fusion in a previous study, increasing potentially the direct oncolytic effect of NDV and cell death in mouse fibroblasts [47]. On the other hand, vanadium compounds have been shown different cellular effects such as ROS formation, regulation of important proteins in the cell cycle activity, cell cycle arrest, DNA damage, and upregulation of p53 [40,48,49]. These effects may also be related to the positive results of the study.

The combination of  $VOSO_4$  at 40 mg/kg and NDV provoked a faster tumor regression in mice, achieving 100% of population survival. On the other hand, vanadyl sulfate alone was able to induce tumor regression and enhance survival of B16-F10. The fact that  $VOSO_4$  in combination with NDV induced a fast tumor regression probably made it impossible to generate enough anti-tumor memory response [27].

### 5.2. XMenes

In Jastrzębska, et al. compound 2,  $V_2CT_z-ox_{24}/V_2CT_z-ox_{48}$  decreased the metabolic activity of A375 and HaCaT cells [26]. The XMenes nanomaterials did not induce apoptosis but the authors related high percentages of necrotic cells in treatments with high concentrations of s- $V_2CT_z-ox_{48}$ .  $V_2CT_z-ox_{24}/V_2CT_z-ox_{48}$  brought cell cycle effects, such as induction of abnormal proliferation potential in A375 cells. Effects on the cell cycle have been described in treatments with 2D materials [50,51] but such effects are not reported on the influence of MXenes. The ROS formation was dependent on the applied dose of the MXenes, in both cell lines. As described previously, both increasing or decreasing mitochondrial membrane potential ( $\Delta\Psi_m$ ) brings negative effects onto cells viability [52–54].

### 5.3. Vanadium Pentoxide

The effects of the compound 3,  $V_2O_5$  have been previously studied in several cell lines, including MDA-MB-231 (human breast cancer cell line), V79 (hamster lung fibroblast cell line), SCCVII (squamous carcinoma cells), FsaR (fibrosarcoma cells), L929 (murine fibroblast cell line) cells and also in B16F10 cells, showing cytotoxicity in all of the examined cell



lines [55,56]. The cytotoxicity in tumor cells led the authors to study  $V_2O_5$  in several other cell lines and in vivo [29]. There was a decrease in the cell viability of the murine melanoma B16F10 cells with increasing doses of vanadium pentoxide. In other cancer cells tested, for example PANC1 (human pancreatic cancer cell) and A549 (human lung carcinoma), treatments resulted in a 35–70% decrease in cell viability, as in B16F10 cells. However, non-cancer fibroblasts or epithelial cells subjected to the same test, HEK-293, CHO and NRK-49F, maintained their normal viability. These results indicate that compound 3,  $V_2O_5$ , could be a potential therapeutic agent against various types of cancer, although not specific for melanoma, having no effect on normal cells viability [29].

Cells treated with  $V_2O_5$  (10  $\mu\text{g}/\text{mL}$ ) and SU-5416, studied through flow cytometry, showed an increase in the apoptotic region compared to untreated cells, suggesting that the compound causes an increase in cell apoptosis [29]. SU-5416 was used as a positive control, as this substance inhibits angiogenesis [38,57]. It was also detected DNA damage, through a TUNEL assay, which exhibited TUNEL positivity with  $V_2O_5$  (10  $\mu\text{g}/\text{mL}$ ) and SU-5416 (20 nM). The generation of  $O_2^-$  (anion superoxide) in the presence of  $V_2O_5$ , in B16F10 cells was also analyzed, and the authors speculated that the generation of  $O_2^-$  would be a plausible mechanism to justify the anti-cancer activity of compound 3.

Additional analysis was carried out to verify the expression of proteins involved in the apoptosis process and to better understand the mechanism of anticancer activity. The results showed a positive regulation of the p53 protein and a negative regulation of the anti-apoptotic survivin protein in cells treated with  $V_2O_5$  (10–20  $\mu\text{g}/\text{mL}$ ) and SU-5416, compared to untreated cells. Since the p53 protein is a tumor suppressor protein and the anti-apoptotic survivin protein is an inhibitor-of-apoptosis protein [58,59], its increase and decrease respectively, validated the anti-cancer potential of  $V_2O_5$  already verified, through cell viability assays. By contrast, it was previously reported that  $V_2O_5$  is harmful to living organisms, as it provokes apoptotic markers in the lung tissues of animals exposed [60].

Before conducting an in vivo experiment with new materials, it is important to check their biocompatibility, being hemocompatibility one important parameter to be analyzed. In Das, et al. the authors analyzed blood taken from the animals, posteriorly treated with compound 3,  $V_2O_5$ , confirming the biocompatible nature of this compound, making in vivo experience possible [29]. After this analysis, the mice were implanted with B16F10 cells and two studies were carried out, one to verify the animals' survival capacity and another to analyze sub chronic toxicity. The results of the first test referred are very positive, showing that with the administration of increasingly higher doses, the longevity of the mice increases. Thus,  $V_2O_5$  triggered mechanisms that allowed the mice to survive longer [29].

In relation to sub chronic toxicity, this experiment served to assess changes in weight and food and water consumption of mice treated with 10 and 20 mg/kg of  $V_2O_5$ , which in turn were not observed, indicating that at the physiological level there are no changes. After sacrifice of the mice that underwent the study of sub chronic toxicity, histopathological analysis was performed. This showed that there were no changes in the organs and only a few changes appeared. According to these results, the authors concluded that there was no toxicity in vital organs, which reinforces the nature biocompatible of the compound 3, vanadium pentoxide, in vivo [29].

Since  $V_2O_5$  is an important catalyst used and produced each year, there is an increasing interest in the biological effects of this material, which has been categorized as a toxic material associated with occupational asthma and compromised pulmonary immune competence [61]. Studies searching the effects of this material are controversial because  $V_2O_5$  materials alter speciation upon dissolution and decavanadate ( $V_{10}$ ) species are observed. Besides, it was proposed that  $V_2O_5$  oxide structurally resembles the  $V_{10}$  species surface [62].  $V_{10}$ , an isopolyoxovanadate, well known inhibitor of key enzymes and also to exert anticancer activities [44], was suggested to target membrane proteins from the extracellular side thus affecting essential cellular processes [63].



#### 5.4. Oxidovanadium(IV) Pyridinonate Compounds

Pisano, et al. published in 2019 [30] is a follow-up of Rozzo, et al. published in 2017 [31], as an attempt to clarify the mechanisms that caused the anticancer effects seen previously. In cell viability assays with compounds 4, 5, 8 and 9 namely VN, VS2, VS3 and VS4, A375, CN-mel melanoma cells and fibroblastic cells were treated [31]. According to the authors, when treated with both 10 and 100  $\mu\text{M}$  concentrations, A375 cells experienced a 98–99.5% decrease in cell viability with all compounds. The authors clearly observed a dose-dependent decrease of cell viability for all compounds and cell lines. The lowest value of cell viability reported corresponds to VS3 treatment in A375 cells, indicating the possibility that this is the compound with the highest anticancer potential against melanoma.

The percentage of apoptotic cells from cells treated with VN and VS2 was also measured [30,31]. In Pisano, et al. [30], percentages of apoptotic cells that were low after 24 h treatments, but after 48 h apoptosis was more evident, indicating that apoptosis depends on the duration of treatments. When NAC was used (inhibitor of ROS formation), there was a decrease in apoptotic cells, confirming that the presence of ROS, due to the use of compounds 4 and 5, VN and VS2, causes cell death. It should be noted that the percentages of apoptotic cells between VN and VS2 did not differ. In Rozzo, et al. [31], the results indicated that treatments lasting 24 h were not sufficient to cause cell death. Only in treatments for 48 h, more relevant results emerged, as in Pisano, et al. The increasing doses were also a factor that contributed to apoptotic effects show up.

The ROS formation by the compounds 4 and 5, VN and VS2 was studied in Pisano, et al. [30] and the results showed that both compounds caused time-dependent ROS production. Concerning to doses, compound 5, VS2 was more dependent on this factor, since there were relevant differences between the treatments with the different doses (10 and 20  $\mu\text{g}/\text{mL}$ ) when treated with this compound, but when treated with VN there were no relevant differences. It should also be noted that after 4 h of treatment, VS2 (in both concentrations 10 and 20  $\mu\text{g}/\text{mL}$ ) showed a higher production of ROS compared to VN. While in the 24 h treatment the situation was inverted and VN caused slightly higher ROS production compared to VS2 (at a concentration of 10  $\mu\text{g}/\text{mL}$ ). In cells treated with NAC, in all concentrations and durations, the percentage of ROS decreased, as expected.

In Rozzo, et al. [31] tests were carried out on A375 cells with compounds 4 and 5, VN and VS2 complexes to evaluate the effects on the cell cycle progression. In the results of 24 h treatments with VN, the percentages of the cell cycle phases changed at the concentration of 20  $\mu\text{g}/\text{mL}$ , where the percentage G0/G1 phase and S phase decrease and the phase G2/M increases, comparing to untreated cells. When treated with VS2, the cell cycle arrested in G0/G1 phase, showing not to be able to enter the S phase. These results indicate that VN interferes with the G2/M cell control point, preventing cells from performing mitosis, while VS2 interferes with the point G0/G1.

In Pisano, et al. [30] it was also studied the phospho-ERK kinase to evaluate the MAPK pathway activation status, with compounds 4 and 5. VN and VS2 showed to neutralize the activation of the MAPK cascade by inducing a dephosphorylation of ERK, contributing to antiproliferative effects in A375 cells. These results diverge from studies already carried out, that show an increase in ERK phosphorylation induced by vanadium compounds in different in vitro models such as in AsPC-1 (human pancreatic cancer), HepG2 (human liver cancer) and in human osteosarcoma cell lines [64–66]. The authors suggested that this ambiguity arises due to the use of melanoma models with V600E BRAF mutation, because this mutation makes the MAPK pathway constitutively active, resulting in ERK hyper-phosphorylation [67].

Retinoblastoma protein (Rb) represents a major role in the control point for the transition from the G1 phase to the S phase. In A375 cell line, VN and VS2 promoted Rb dephosphorylation, preventing cell cycle progression, once Rb dephosphorylation mitigates the effects of CDKN2A mutations, which exist in the cells studied [68]. Such effects also appeared in a study with human pancreatic cancer AsPC-1 cells [64]. The cyclin/CDK complex inhibitor p21Cip1 increased with treatments with VN and VS2, as expected, since

upregulation of p21Cip1 is associated with cell cycle arrest and apoptosis, in response to p53 activation [69]. It was studied the cell division cycle 25C phosphatase Cdc25C, which plays a key role in the transition from phase G2 to phase M, by its activation, but the results excluded Cdc25C phosphatase from being involved in cell cycle arrest in G2 phase.

### 5.5. Polysaccharides Vanadium(IV/V) Complexes

Polysaccharides and vanadium compounds have been studied due to their anticancer effects [70]. In one of the selected articles, it was particularly studied the effects of xyloglucan from *Copaifera langsdorffii* complexed with oxovanadium [32]. Polysaccharides complexed with oxovanadium already showed cytotoxic effects in another study carried out on human hepatocarcinoma (HepG2) cells, subjected to treatments with galactomannan polysaccharide of *Schizolobium amazonicum* seeds [70]. The polysaccharide XGC (xyloglucan) is extracted from *Copaifera langsdorffii* seeds and this fruit has been shown antimutagenic and antitumor properties, as well as ability to deliver medications [71–73]. Both XGC and the compound 6, XGC:VO, showed cytotoxicity to B16F10 cells, dose-dependent, observing that the higher dose caused the lower cell viability, assessed through MTT assays. This suggests that both XGC and compound 6 could be potential anticancer agents against melanoma due to the presence of the polysaccharide XGC and not necessarily due to the use of vanadium, since the presence or absence of it does not bring relevant differences in terms of cell viability. B16F10 cells proliferation was evaluated through trypan blue exclusion method and it was found similar effects as in the MTT assay, except the fact that cells treated with compound 6 showed slightly lower percentages of cell viability than cells treated with XGC solo, suggesting some effect specifically derived from vanadium [32].

Treatment with compound 6 and XGC was not able to induce cell death at concentrations of 5 and 20 µg/mL [32]. However, incubation with 200 µg/mL of compound 6 increased the number of apoptotic cells, compared to the control. This result suggests that the presence of the metal was crucial for the induction of apoptosis, since in the presence of XGC only, the number of apoptotic cells did not increase. These results contradict the results of cell viability, which suggest that the presence of vanadium is useless.

Additionally, the treatment with xyloglucan alone and with compound 6, was not able to change the cell cycle of B16F10 cells. In the other hand, treatments with compound 6 resulted in the inhibition of respiration of B16F10 cells. It has been previously described that vanadium compounds, namely decavanadate, induces mitochondrial membrane depolarization and inhibits oxygen consumption in rat liver [74]. This decrease in cells respiration with compound 6, may also be related to the decrease of pyruvate levels, that were also reported in this study. Similar effects, such as decreased cellular respiration and pyruvate levels, were also reported in the study in HepG2 cells incubated with galactomannose-oxovanadium complexes [70].

### 5.6. Mixed-Metal Binuclear Ruthenium(II)–Vanadium(IV) Complexes

Recently, studies have been carried out involving photodynamic therapy and vanadium complexes [75,76]. In Holder, et al. [34], the elements ruthenium and vanadium were used as photodynamic therapy agents, in association with other constituents. These other constituents, VO(sal-L-tryp) for example, are related to DNA photo-cleavage [77,78]. It was evaluated the effects on the morphology and cell death of human amelanotic malignant melanoma cells treated with the compound 10 Ru-(pbt)<sub>2</sub>(tpphz)VO(sal-L-tryp)Cl<sub>2</sub>, a mixed-metal binuclear ruthenium(II)–vanadium(IV) complexes and the results showed that the cytotoxicity of the compound was dose- and light-dependent. In the presence of light, and at the highest concentration (20 µM), the most pronounced effects were observed (appearance of apoptosis). Fibroblastic cells that were also subjected to the same treatment, showed no changes, suggesting that there are no effects on healthy normal cells.

### 5.7. Pyridoxal-Based Oxidovanadium(IV) Complexes

In Strianese, et al. Pyr<sub>2</sub>en was selected to be complexed with vanadium since it is a form of vitamin B6, being a non-toxic cofactor required by several enzymes [35]. In A375 cells, compound **11**, a pyridoxal-based oxidovanadium(IV) complex, reduced the cell viability by 93% in a concentration of 50 µM (the only one used), indicating a potential anti-cancer effect of vanadium in these cells, since with Pyr<sub>2</sub>en ligand (without vanadium), the decrease was only 18%. In other cancer cell lines tested, the complex only decreased cell viability in A549 (human lung carcinoma) and HT29 (human colon adenocarcinoma) cells, but not as expressively as in A375 melanoma cells, having no effects on MCF7 (human breast adenocarcinoma), H69 (human small cell lung cancer) and U266 (human multiple myeloma) cells. Regarding non-cancerous cell lines, compound **11**, Pyr<sub>2</sub>enVO, caused a 20% and 32% decrease in cell viability on NEK (normal human epidermal keratinocytes) and NuLi (normal lung cells) cells, respectively, while in PBMC (peripheral blood mononuclear cells) cells there were no changes in cell viability. These results suggest that compound **11** may be used as an anticancer agent in melanoma, as it indicates some specificity for this type of cancer.

For compound **11**, the percentage of apoptotic nuclei sub-G0/G1 was measured in A375 and A549 cells. These percentages increased with increasing concentrations of the compound and the duration of treatments in A375 cells, while in A549 cells no increase was observed. These results indicate that compound **11** induced cell cycle arrest in the G0/G1 phase specifically in melanoma cells. The cell cycle was interrupted in an initial phase, preventing the progression of tumor cells [35]. This effect on cell cycle has already been reported in B16F10 cells treated with ethanolic extract of *Aerva lanata* [79].

Regarding the measurement of the percentage of ROS, the cells treated with Pyr<sub>2</sub>en solo, showed almost zero ROS formation (always less than or equal to 2%). Cells treated with compound **11** had low ROS percentages (always less than or equal to 23%), but it appeared to be dependent on the duration and presence/absence of NAC, as in the presence of this inhibitor the percentages of ROS are almost zero (1–3%). In another study, azosalene complexes with oxidovanadium(IV) in A549 cells showed cytotoxicity, leading to apoptosis by the formation of ROS, suggesting that this effect is common with this form of vanadium [80]. The authors considered that the appearance of ROS was followed by the depolarization of the mitochondrial membrane, which was also reported [35].

### 5.8. Nanoparticles of Yttrium Vanadate Doped with Europium

The effects of cisplatin (CDDP) have been extensively studied over the years due to its anti-tumor potential, but due to its systemic toxicity, the goal is to find a compound that does not diminish its potential anticancer but that reduces the adverse systemic effects [81]. One of the selected articles studied this possibility, more concretely the possibility of Y<sup>III</sup>V<sup>V</sup>O<sub>4</sub>:Eu<sup>III</sup> to reduce systemic toxicity, though not decreasing the anticancer action, of cisplatin [33]. Nanoparticles of yttrium vanadate doped with europium were used isolated and functionalized with CPTES (3-chloropropyltrimethoxysilane), FA (folic acid) and with CDDP, compound **7**. The use of folic acid (FA) with nanoparticles, in therapies against cancer, helps in therapy targeting, once FA binds to FR (folate receptor), which is overexpressed in cancer cells [82]. After the mice were injected with B16F10 cells, the body weight of the animals and the tumor volume (calculated using a specific equation), were controlled during the 5 days of the study. The results indicated that the complex with Y<sup>III</sup>V<sup>V</sup>O<sub>4</sub>:Eu<sup>III</sup>, compound **7**, caused a relevant decrease in tumor weight, in the presence of CDDP. The authors also found that all animals that survived treatments with CDDP alone (only 70% of the group survived), showed signs of systemic toxicity such as hair loss, dehydration, weight loss and reduced activity. The same was not true in the groups treated with Y<sup>III</sup>V<sup>V</sup>O<sub>4</sub>:Eu<sup>III</sup>:CPTES:CDDP and Y<sup>III</sup>V<sup>V</sup>O<sub>4</sub>:Eu<sup>III</sup>:CPTES:FA:CDDP. While the anticancer effect is attributed to cisplatin, the use of Y<sup>III</sup>V<sup>V</sup>O<sub>4</sub>:Eu<sup>III</sup> showed to decrease its systemic toxicity.

Cisplatin's toxicity has been one of the problems of its use, since it makes its application *in vivo* difficult [83]. However, more studies are emerging about the anti-cancer potential of CDDP derivatives, in order to reduce systemic toxicity, and studies on B16F10 cells have already been published for instance with oxaliplatin (OXA) [84]. After mice's sacrifice, several analyzes were carried out, namely a histopathological analysis, where it was found that only changes in cell proliferation occur when the mice are treated with doses of  $Y^{III}V^VO_4:Eu^{III}$  that include CDDP, indicating that vanadium is not primarily responsible for cell proliferation decreasing rather cisplatin, as previously described. Results from a micronucleus assay, which assesses the frequency of micronuclei, indicators of genotoxic damage [85], showed that there was a greater formation of micronuclei in animals treated with  $Y^{III}V^VO_4:Eu^{III}:CPTES:CDDP$ , in relation to all other compounds suggesting that FA may have helped in decreasing genotoxicity [33].

## 6. Conclusions

In sum, herein it is described recent studies for eleven vanadium species, compounds and materials, in several human melanoma cells lines. Vanadium compounds with anticancer activity against melanoma include: (1) oxidovanadium (IV) (compound 1); (2) XMenes (compound 2); (3) vanadium pentoxide (compound 3); (4) vanadate (compound 4); (5) oxidovanadium(IV) pyridinonate compounds (compound 5, 7 and 8); (6) polysaccharides vanadium(IV/V) complexes (compound 6); (7) functionalized nanoparticles of yttrium vanadate doped with europium (compound 7); (8) mixed-metal binuclear ruthenium(II)–vanadium(IV) complexes (compound 10); and (9) pyridoxal-based oxidovanadium(IV) complexes (compound 11). The effects of vanadium in melanoma were reported in several human melanoma cell lines such as A375, CN-mel and amelanotic melanoma, and murine skin melanoma B16F10 cells, although *in vivo* mice studies were also described. The effects described for the eleven vanadium compounds analyzed include: (1) cell viability; (2) cell morphology changes and apoptosis; (3) cell cycle; (4) ROS production; (5) mitochondrial dysfunction; (6) proteins expression; and (7) *in vivo* tumor regression and survival rates (Figure 3).

The vanadium compounds/materials relative order for cell inhibition potency, is dependent of cancer cells' types. For example, for CN-mel cells vanadate was found to be more potent than all the oxidovanadium(IV) pyridinonate compounds, whereas the opposite happens regarding A375 cells. The cell cycle effects induced by vanadate, oxidovanadium(IV) pyridinonate compounds, XMenes and pyridoxal-based oxidovanadium(IV) complexes; the ROS production induced by the majority of the vanadium compounds; the mitochondrial respiration inhibition observed for polysaccharides vanadium(IV/V) complexes and the membrane potential affected by XMenes and pyridoxal-based oxidovanadium(IV) complexes; the changes in protein expression by vanadate and oxidovanadium(IV) pyridinonate compounds; and finally, the oxidovanadium (IV) *in vivo* synergies with the oncolytic virus NDV in promoting tumor regression, as well as the increasing of survival rates observed for mixed-metal binuclear ruthenium(II)–vanadium(IV) complexes and vanadium pentoxide without toxicity effects in vital organs described for the former, point out for a useful approach to treat melanoma. Moreover, the nanoparticles of yttrium vanadate doped with europium functionalized with CPTES, FA and CDDP, showed to be a good strategy to, besides preventing the toxicity of cisplatin, potentiate the effects of the major and well-known metal drug against cancer.

These studies demonstrate that such vanadium applications in melanoma are possible. Only a few pre-clinical models of cancer have been carried out with vanadium so far [27], although much work has been carried out with vanadium compounds, suggesting a potential therapeutic opportunity. Such studies are demanding and require interdisciplinary teams to develop new vanadium materials and/or complexes [86], and to select which vanadium is suited for further development against a particular disease. In the present decade, we expect that important questions will be answered, in order to push forward the practice of metals compounds—particularly, vanadium—for the treatment of cancer.

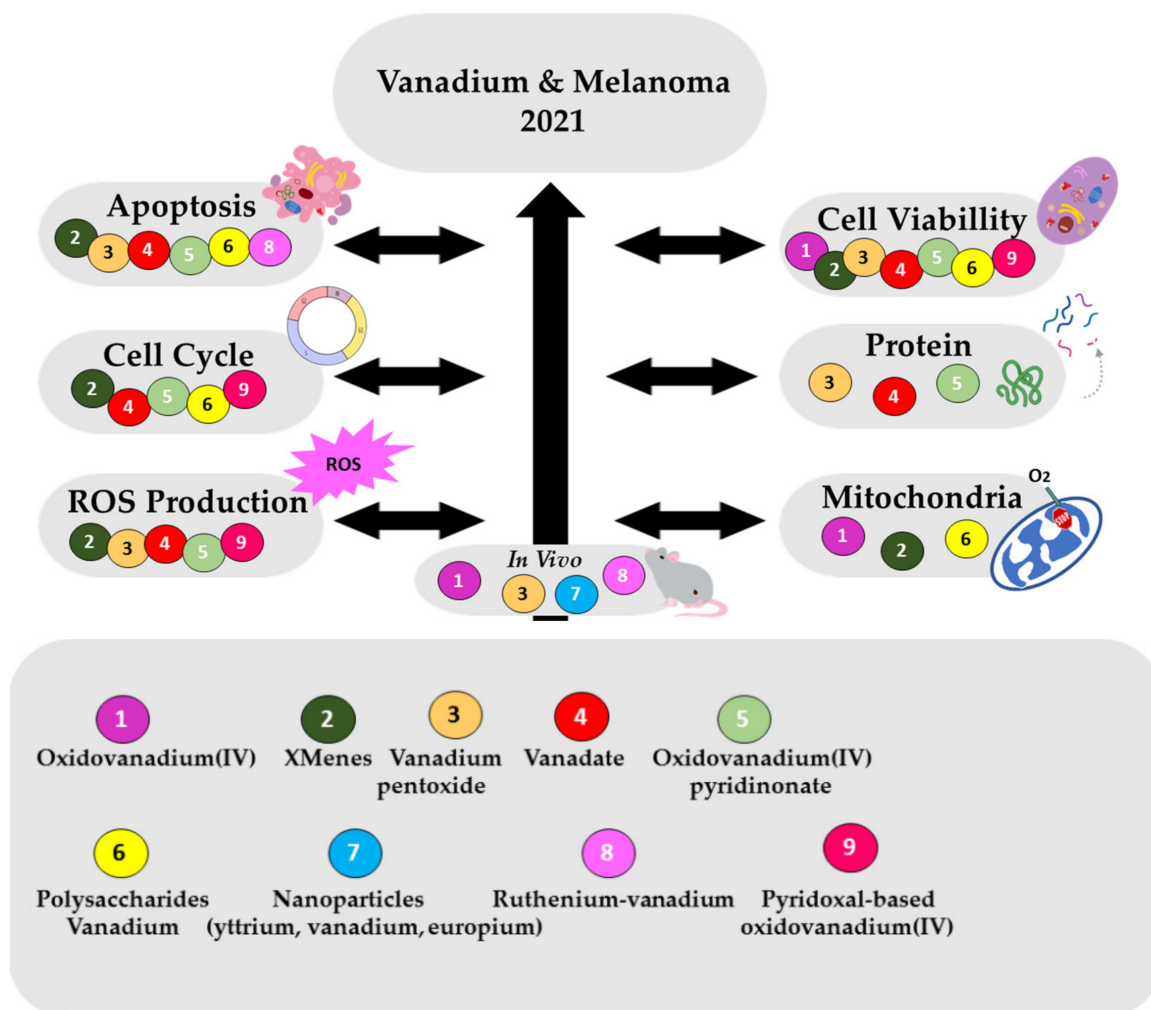


**Figure 3.** Distribution of the vanadium compounds regarding the effects described in melanoma include: cell viability, apoptosis and morphology changes; cell cycle arrest, ROS production, mitochondria dysfunction; proteins expression and in vivo tumor regression and rate of survival studies. Billiard balls representing the vanadium compounds: (1) oxidovanadium (IV); (2) XMenes; (3) vanadium pentoxide; (4) vanadate; (5) oxidovanadium(IV) pyridinonate compounds; (6) polysaccharides vanadium(IV/V) complexes; (7) functionalized nanoparticles of yttrium vanadate doped with europium; (8) mixed-metal binuclear ruthenium(II)–vanadium(IV) complexes; (9) pyridoxal-based oxidovanadium(IV) complexes.

**Author Contributions:** Conceptualization, A.L.D.S.-C. and M.A.; formal analysis, C.A., A.L.D.S.-C. and M.A.; funding acquisition, M.A.; investigation, C.A., A.L.D.S.-C. and M.A.; methodology, C.A., A.L.D.S.-C. and M.A.; supervision, A.L.D.S.-C. and M.A.; writing—original draft, C.A., A.L.D.S.-C. and M.A.; writing—review and editing, C.A., A.L.D.S.-C. and M.A. All authors have read and agreed to the published version of the manuscript.

**Funding:** The authors acknowledge Fundação para a Ciência e Tecnologia (FCT) for the project UIDB/04326/2020.

**Institutional Review Board Statement:** Not applicable.

**Informed Consent Statement:** Not applicable.

**Data Availability Statement:** Not applicable.

**Conflicts of Interest:** The authors declare no conflict of interest.



## Abbreviations

A375	human malignant melanoma
A549	human lung carcinoma
ARID2	AT-rich interaction domain 2
AsPC-1	human pancreatic cancer
B16F10	mus musculus skin melanoma
BRAF	B-Raf proto-oncogene
CDDP	cisplatin or cis-diamminedichloroplatinum(II)
CDK	cyclin dependent kinase
CDKN2A	cyclin-dependent kinase inhibitor 2A
CHO	chinese hamster ovary cells
CN-mel	human noncutaneous metastatic melanoma
CPTES	3-chloropropyltrimethoxysilane
DCF-DA	fluorescent dye
DHE	dihydroethidium
$\Delta\Psi_m$	mitochondrial membrane potential
ERK	extracellular signal-regulated kinase
FA	folic acid
FITC	fluorescein isothiocyanate
FR	folate receptor
FSaR	fibrosarcoma cells
H69	human small cell lung cancer
HaCaT	immortalized keratinocytes
HAM-F10	F-10 nutrient medium
HDL	high density lipoprotein
HEK-293	human embryonic cells
HepG2	human hepatocarcinoma
HT29	human colon adenocarcinoma
IFN- $\gamma$	interferon gamma
KIT	KIT proto-oncogene receptor tyrosine kinase
LDL	low density lipoprotein
L929	murine fibroblasts
MAPK	mitogen-activated protein kinase
MC1R	melanocortin 1 receptor
MDA-MB 231	breast adenocarcinoma
MCF7	human breast cancer
MOI	multiplicity of infection
MSH	melanocyte stimulating hormone
MTT	[3-(4,5-dimethylthiazol-2-yl)-2,5-diphenyltetrazolium bromide]
Na <sup>+</sup> /K <sup>+</sup> -ATPase	Na <sup>+</sup> /K <sup>+</sup> pump ATP dependent
NAC	N-acetylcysteine
NDV	Newcastle disease virus
NEK	normal human epidermal keratinocytes
NF1	neurofibromin 1
NRK-49F	rat kidney cell line
NPs	nanoparticles
NuLi	normal lung cells
O <sub>2</sub> <sup>-</sup>	anion superoxide
PANC1	human pancreatic cancer cells
PARP	Poly (ADP-ribose) polymerase
PBMC	peripheral blood mononuclear cells
PBS	phosphate buffer
ph-Rb	phosphorylated retinoblastoma protein
PI	propidium iodide
PIK3CA	phosphatidylinositol-4,5-bisphosphate 3-kinase catalytic subunit alpha
POTs	polyoxotungstates



PTEN	phosphatase and tensin homolog
Pyr2enVO	N,N'-ethylenebis (pyridoxylideneiminat) vanadium(IV)
Rb	retinoblastoma protein
ROS	reactive oxygen species
RuVO	[Ru-(pbt) <sub>2</sub> (tpphz)VO(sal-L-tryp)]Cl <sub>2</sub>
SCCVII	squamous carcinoma cells
SU-5416	semaxanib
TdLNs	tumor-draining lymph nodes
TERT	telomerase reverse transcriptase
TME	tumor microenvironment
TP53	tumor protein p53
U266	human multiple myeloma
VN	monomeric vanadate
V79	hamster lung fibroblast cell line
VO	oxidovanadium (IV)
VOSO <sub>4</sub>	vanadyl sulphate
VP	Vanadium pentoxide
VS2	[VIVO(dhp) <sub>2</sub> ], 1,2-dimethyl-3-hydroxy-4(1H)-pyridinonate
VS3	[VIVO(mpp) <sub>2</sub> ], mpp: 1-methyl-3-hydroxy-4(1H) pyridinonate
VS4	[VIVO(ppp) <sub>2</sub> ], ppp: 1-phenyl-2-methyl-3-hydroxy-4(1H)-pyridinonate
W10	decatungstate
XGC	Xyloglucan
XGC:VO	Xyloglucan oxovanadium
XMenes	transition metal carbides/nitrides

## References

- Mondal, A.H.; Behera, T.; Swain, P.; Das, R.; Sahoo, S.N.; Mishra, S.S.; Das, J.; Ghosh, K. Nano zinc vis-à-vis inorganic Zinc as feed additives: Effects on growth, activity of hepatic enzymes and non-specific immunity in rohu, *Labeo rohita* (Hamilton) fingerlings. *Aquac. Nutr.* **2020**, *26*, 1211–1222. [[CrossRef](#)]
- Yan, S.; Wu, F.; Zhou, S.; Yang, J.; Tang, X.; Ye, W. Zinc oxide nanoparticles alleviate the arsenic toxicity and decrease the accumulation of arsenic in rice (*Oryza Sativa* L.). *BMC Plant Biol.* **2021**, *21*, 150. [[CrossRef](#)]
- Carofiglio, M.; Barui, S.; Cauda, V.; Laurenti, M. Doped zinc oxide nanoparticles: Synthesis, characterization and potential use in nanomedicine. *Appl. Sci.* **2020**, *10*, 5194. [[CrossRef](#)]
- Arentz, S.; Hunter, J.; Yang, G.; Goldenberg, J.; Beardsley, J.; Myers, S.P.; Mertz, D.; Leeder, S. Zinc for the prevention and treatment of SARS-CoV-2 and other acute viral respiratory infections: A rapid review. *Adv. Integr. Med.* **2020**, *7*, 252–260. [[CrossRef](#)]
- Cheng, P.; Wang, Y.; Sarakha, M.; Mailhot, G. Enhancement of the photocatalytic activity of decatungstate, W<sub>10</sub>O<sub>32</sub>–, for the oxidation of sulfasalazine/sulfapyridine in the presence of hydrogen peroxide. *J. Photochem. Photobiol. A Chem.* **2021**, *404*, 112890. [[CrossRef](#)]
- Pimpão, C.; da Silva, I.V.; Mósca, A.F.; Pinho, J.O.; Gaspar, M.M.; Gumerova, N.I.; Rompel, A.; Aureliano, M.; Soveral, G. The aquaporin-3-inhibiting potential of polyoxotungstates. *Int. J. Mol. Sci.* **2020**, *21*, 2467. [[CrossRef](#)] [[PubMed](#)]
- Gumerova, N.; Krivosudsky, L.; Fraqueza, G.; Breibeck, J.; Al-Sayed, E.; Tanuhadi, E.; Bijelic, A.; Fuentes, J.; Aureliano, M.; Rompel, A. The P-type ATPase inhibiting potential of polyoxotungstates. *Metallomics* **2018**, *10*, 287–295. [[CrossRef](#)]
- Fonseca, C.; Fraqueza, G.; Carabineiro, S.A.C.; Aureliano, M. The Ca<sup>2+</sup>-ATPase inhibition potential of gold (I,III) compounds. *Inorganics* **2020**, *8*, 49. [[CrossRef](#)]
- Li, P.; Chen, P.; Wang, G.; Wang, L.; Wang, X.; Li, Y.; Zhang, W.; Jiang, H.; Chen, H. Uranium elimination and recovery from wastewater with ligand chelation-enhanced electrocoagulation. *Chem. Eng. J.* **2020**, *393*, 124819. [[CrossRef](#)]
- Vijaya, P.; Kaur, H.; Garg, N.; Sharma, S. Protective and therapeutic effects of garlic and tomato on cadmium-induced neuropathology in mice. *J. Basic Appl. Zool.* **2020**, *81*, 23. [[CrossRef](#)]
- Obeng-Gyasi, E. Chronic cadmium exposure and cardiovascular disease in adults. *J. Environ. Sci. Health Part A* **2020**, *55*, 726–729. [[CrossRef](#)] [[PubMed](#)]
- Vosahlikova, M.; Roubalova, L.; Cechova, K.; Kaufman, J.; Musil, S.; Miksik, I.; Alda, M.; Svoboda, P. Na<sup>+</sup>/K<sup>+</sup>-ATPase and lipid peroxidation in forebrain cortex and hippocampus of sleep-deprived rats treated with therapeutic lithium concentration for different periods of time. *Prog. Neuro Psychopharmacol. Biol. Psychiatry* **2020**, *102*, 109953. [[CrossRef](#)] [[PubMed](#)]
- Hossein-zadeh, Z.; Hauser, S.; Singh, Y.; Pelzl, L.; Schuster, S.; Sharma, Y.; Höflinger, P.; Zacharopoulou, N.; Stournaras, C.; Rathbun, D.L.; et al. Decreased Na<sup>+</sup>/K<sup>+</sup> ATPase expression and depolarized cell membrane in neurons differentiated from chorea-acanthocytosis patients. *Sci. Rep.* **2020**, *10*, 8391. [[CrossRef](#)] [[PubMed](#)]
- Gómez-Arnaiz, S.; Tate, R.J.; Grant, M.H. Cytotoxicity of cobalt chloride in brain cell lines—A comparison between astrocytoma and neuroblastoma cells. *Toxicol. Vitro* **2020**, *68*, 104958. [[CrossRef](#)]

15. Bejarbaneh, M.; Moradi-Shoeili, Z.; Jalali, A.; Salehzadeh, A. Synthesis of cobalt hydroxide nano-flakes functionalized with glutamic acid and conjugated with thiosemicarbazide for anticancer activities against human breast cancer cells. *Biol. Trace Elem. Res.* **2020**, *198*, 98–108. [[CrossRef](#)]
16. Treviño, S.; Díaz, A.; Sánchez-Lara, E.; Sanchez-Gaytan, B.L.; Perez-Aguilar, J.M.; González-Vergara, E. Vanadium in biological action: Chemical, pharmacological aspects, and metabolic implications in diabetes mellitus. *Biol. Trace Elem. Res.* **2019**, *188*, 68–98. [[CrossRef](#)]
17. Sánchez-Lara, E.; Treviño, S.; Sánchez-Gaytán, B.L.; Sánchez-Mora, E.; Castro, M.E.; Meléndez-Bustamante, F.J.; Méndez-Rojas, M.A.; González-Vergara, E. Decavanadate salts of cytosine and metformin: A combined experimental-theoretical study of potential metallodrugs against diabetes and cancer. *Front. Chem.* **2018**, *6*, 402. [[CrossRef](#)]
18. Zhang, Q.K.; Yue, C.P.; Zhang, Y.; Lu, Y.; Hao, Y.P.; Miao, Y.L.; Li, J.P.; Liu, Z.Y. Six metal-organic frameworks assembled from asymmetric triazole carboxylate ligands: Synthesis, crystal structures, photoluminescence properties and antibacterial activities. *Inorg. Chim. Acta* **2018**, *473*, 112–120. [[CrossRef](#)]
19. Wang, X.T.; Li, R.Y.; Liu, A.G.; Yue, C.P.; Wang, S.M.; Cheng, J.J.; Li, J.P.; Liu, Z.Y. Syntheses, crystal structures, antibacterial activities of Cu (II) and Ni (II) complexes based on terpyridine polycarboxylic acid ligand. *J. Mol. Struct.* **2019**, *1184*, 503–511. [[CrossRef](#)]
20. Leonardi, G.C.; Falzone, L.; Salemi, R.; Zanghi, A.; Spandidos, D.A.; Mccubrey, J.A.; Candido, S.; Libra, M. Cutaneous melanoma: From pathogenesis to therapy. *Int. J. Oncol.* **2018**, *52*, 1071–1080. [[CrossRef](#)]
21. Rastrelli, M.; Tropea, S.; Rossi, C.R.; Alaibac, M. Melanoma: Epidemiology, risk factors, pathogenesis, diagnosis and classification. *Vivo* **2014**, *28*, 1005–1011, PMID: 25398793. [[PubMed](#)]
22. Luke, J.J.; Flaherty, K.T.; Ribas, A.; Long, G.V. Targeted agents and immunotherapies: Optimizing outcomes in melanoma. *Nat. Rev. Clin. Oncol.* **2017**, *14*, 463–482. [[CrossRef](#)] [[PubMed](#)]
23. Paluncic, J.; Kovacevic, Z.; Jansson, P.J.; Kalinowski, D.; Merlot, A.M.; Huang, M.L.-H.; Sahni, S.; Lane, D.J.R.; Richardson, D.R. Roads to melanoma: Key pathways and emerging players in melanoma progression and oncogenic signaling. *Biochim. Biophys. Acta* **2016**, *1863*, 770–784. [[CrossRef](#)] [[PubMed](#)]
24. Grayschopfer, V.; Wellbrock, C.; Marais, R. Melanoma biology and new targeted therapy. *Nature* **2007**, *445*, 851–857. [[CrossRef](#)] [[PubMed](#)]
25. Ali, Z.; Yousaf, N.; Larkin, J. Melanoma epidemiology, biology and prognosis. *Eur. J. Cancer Suppl.* **2013**, *11*, 81–91. [[CrossRef](#)] [[PubMed](#)]
26. Srinivasan, A.; Toh, Y. Human pluripotent stem cell-derived neural crest cells for tissue regeneration and disease modeling. *Front. Mol. Neurosci.* **2019**, *12*, 39. [[CrossRef](#)]
27. Mcausland, T.M.; Vloten, J.P.V.; Santry, L.A.; Guilleman, M.M.; Rghei, A.D.; Ferreira, E.M.; Ingraio, J.C.; Arulanandam, R.; Major, P.P.; Susta, L.; et al. Combining vanadyl sulfate with Newcastle disease virus potentiates rapid innate immune-mediated regression with curative potential in murine cancer models. *Mol. Ther. Oncolytics* **2021**, *20*, 306–324. [[CrossRef](#)]
28. Jastrzębska, A.M.; Scheibe, B.; Szuplewska, A.; Rozmysłowska-Wojciechowska, A.; Chudy, M.; Aparicio, C.; Scheibe, M.; Janica, I.; Ciesielski, A.; Otyepka, M.; et al. On the rapid in situ oxidation of two-dimensional V<sub>2</sub>CT<sub>z</sub> MXene in culture cell media and their cytotoxicity. *Mater. Sci. Eng. C* **2021**, *119*, 111431. [[CrossRef](#)] [[PubMed](#)]
29. Das, S.; Roy, A.; Barui, A.K.; Alabbasi, M.M.A.; Kuncha, M.; Sistla, R.; Sreedhar, B.; Patra, C.R. Anti-angiogenic vanadium pentoxide nanoparticles for the treatment of melanoma and their in vivo toxicity study. *Nanoscale* **2020**, *12*, 7604–7621. [[CrossRef](#)]
30. Pisano, M.; Arru, C.; Serra, M.; Galleri, G.; Sanna, D.; Garribba, E.; Palmieri, G.; Rozzo, C. Antiproliferative activity of vanadium compounds: Effects on the major malignant melanoma molecular pathways. *Metallomics* **2019**, *11*, 1687–1699. [[CrossRef](#)]
31. Rozzo, C.; Sanna, D.; Garribba, E.; Serra, M.; Cantara, A.; Palmieri, G.; Pisano, M. Antitumoral effect of vanadium compounds in malignant melanoma cell lines. *J. Inorg. Biochem.* **2017**, *174*, 14–24. [[CrossRef](#)] [[PubMed](#)]
32. Farias, C.L.A.; Martinez, G.R.; Cadena, S.M.S.C.; Mercê, A.L.R.; Petkowicz, C.L.; Noleto, G.R. Cytotoxicity of xyloglucan from *Copaifera langsdorffii* and its complex with oxovanadium (IV/V) on B16F10 cells. *Int. J. Biol. Macromol.* **2018**, *121*, 1019–1028. [[CrossRef](#)] [[PubMed](#)]
33. Ferreira, N.H.; Furtado, R.A.; Ribeiro, A.B.; Oliveira, P.F.; Ozelin, S.D.; Souza, L.D.R.; Neto, F.R.; Miura, B.A.; Magalhães, G.M.; Nassar, E.J.; et al. Europium (III)—Doped yttrium vanadate nanoparticles reduce the toxicity of cisplatin. *J. Inorg. Biochem.* **2018**, *182*, 9–17. [[CrossRef](#)] [[PubMed](#)]
34. Holder, A.A.; Taylor, P.; Magnusen, A.R.; Moffett, E.T.; Meyer, K.; Hong, Y.; Ramsdale, S.E.; Gordon, M.; Stubbs, J.; Seymour, L.A.; et al. Preliminary anti-cancer photodynamic therapeutic in vitro studies with mixed-metal binuclear ruthenium (II)–vanadium (IV) complexes. *Dalton Trans.* **2013**, *42*, 11881–11899. [[CrossRef](#)] [[PubMed](#)]
35. Strianese, M.; Basile, A.; Mazzone, A.; Morello, S.; Turco, M.C.; Pellicchia, C. Therapeutic potential of a pyridoxal-based vanadium (IV) complex showing selective cytotoxicity for cancer vs. healthy cells. *J. Cell. Physiol.* **2013**, *228*, 2202–2209. [[CrossRef](#)]
36. Burman, B.; Pesci, G.; Zamarin, D. Newcastle disease virus at the forefront of cancer immunotherapy. *Cancers* **2020**, *12*, 3552. [[CrossRef](#)]
37. Lacal, P.M.; Failla, C.M.; Pagani, E.; Odorisio, T.; Schietroma, C.; Falcinelli, S.; Zambruno, G.; D’Atr, S. Human melanoma cells secrete and respond to placenta growth factor and vascular endothelial growth factor. *J. Investig. Dermatol.* **2000**, *115*, 1000–1007. [[CrossRef](#)]

38. Ogawara, K.; Abe, S.; Un, K.; Yoshizawa, Y.; Kimura, T.; Higaki, K. Determinants for in vivo antitumor effect of angiogenesis inhibitor SU5416 formulated in PEGylated emulsion. *J. Pharm. Sci.* **2014**, *103*, 2464–2469. [[CrossRef](#)]
39. Aldini, G.; Altomare, A.; Baron, G.; Vistoli, G.; Carini, M.; Borsani, L.; Sergio, F. N-Acetylcysteine as an antioxidant and disulphide breaking agent: The reasons why. *Free Radic. Res.* **2018**, *52*, 751–762. [[CrossRef](#)]
40. Scibior, A.; Pietrzyk, L.; Plewa, Z.; Skiba, A. Vanadium: Risks and possible benefits in the light of a comprehensive overview of its pharmacotoxicological mechanisms and multi-applications with a summary of further research trends. *J. Trace. Elem. Med. Biol.* **2020**, *61*. [[CrossRef](#)]
41. Evangelou, A.M. Vanadium in cancer treatment. *Crit. Rev. Oncol. Hematol.* **2002**, *42*, 249–265. [[CrossRef](#)]
42. Pessoa, J.C.; Etcheverry, S.; Gambino, D. Vanadium compounds in medicine. *Coord. Chem. Rev.* **2015**, *301*, 24–48. [[CrossRef](#)] [[PubMed](#)]
43. Barrio, D.A.; Etcheverry, S.B. Potential use of vanadium compounds in therapeutics. *Curr. Med. Chem.* **2010**, *17*, 3632–3642. [[CrossRef](#)]
44. Bijelic, A.; Aureliano, M.; Rompel, A. Polyoxometalates as potential next-generation metallodrugs in the combat against cancer. *Angew. Chem. Int. Ed. Engl.* **2019**, *58*, 2980–2999. [[CrossRef](#)]
45. Bijelic, A.; Aureliano, M.; Rompel, A. The antibacterial activity of polyoxometalates: Structures, antibiotic effects and future perspectives. *Chem. Commun.* **2018**, *54*, 1153–1169. [[CrossRef](#)]
46. Imbert, V.; Rupec, R.A.; Livolsi, A.; Pahl, H.L.; Traenckner, E.B.; Mueller-Dieckmann, C.; Farahifar, D.; Rossi, B.; Auberger, P.; Baeuerle, P.A.; et al. Tyrosine phosphorylation of I kappa B-alpha activates NF-kappa B without proteolytic degradation of I kappa B-alpha. *Cell* **1996**, *86*, 787–798. [[CrossRef](#)]
47. Yamamoto, F.; Fujioka, H.; Iinuma, M.; Takano, M.; Maeno, K.; Nagai, Y.; Ito, Y. Enhancement of Newcastle disease virus-induced fusion of mouse L Cells by sodium vanadate. *Microbiol. Immun.* **1984**, *28*, 75–83. [[CrossRef](#)] [[PubMed](#)]
48. Korbecki, J.; Baranowska-Bosiacka, I.; Gutowska, I.; Chlubek, D. Biochemical and medical importance of vanadium compounds. *Acta Biochim. Pol.* **2012**, *59*, 195–200. [[CrossRef](#)]
49. Rojas, E.; Valverde, M.; Herrera, L.A.; Altamirano-lozano, M.; Ostrosky-Wegman, P. Genotoxicity of vanadium pentoxide evaluate by the single cell gel electrophoresis assay in human lymphocytes. *Mutat. Res.* **1996**, *359*, 77–84. [[CrossRef](#)]
50. Kang, Y.; Liu, J.; Wu, J.; Yin, Q.; Liang, H.; Chen, A.; Shao, L. Graphene oxide and reduced graphene oxide induced neural pheochromocytoma-derived PC12 cell lines apoptosis and cell cycle alterations via the ERK signaling pathways. *Int. J. Nanomed.* **2017**, *12*, 5501–5510. [[CrossRef](#)]
51. Nandi, A.; Ghosh, C.; Bajpai, A.; Basu, S. Graphene oxide nanocells for impairing topoisomerase and DNA in cancer cells. *J. Mater. Chem. B* **2019**, *7*, 4191–4197. [[CrossRef](#)]
52. Pérez-Torres, I.; Guarner-Lans, V.; Rubio-Ruiz, M.E. Reductive stress in inflammation-associated diseases and the pro-oxidant effect of antioxidant agents. *Int. J. Mol. Sci.* **2017**, *18*, 2098. [[CrossRef](#)] [[PubMed](#)]
53. Skulachev, V.P. Role of uncoupled and non-coupled oxidations in maintenance of safely low levels of oxygen and its one-electron reductants. *Q. Rev. Biophys.* **1996**, *29*, 169–202. [[CrossRef](#)] [[PubMed](#)]
54. Starkov, A.A.; Fiskum, G. Regulation of brain mitochondrial H<sub>2</sub>O<sub>2</sub> production by membrane potential and NAD (P) H redox state. *J. Neurochem.* **2003**, *86*, 1101–1107. [[CrossRef](#)] [[PubMed](#)]
55. Suma, P.R.P.; Padmanabhan, R.A.; Telukutla, S.R.; Ravindran, R.; Velikkakath, A.K.G.; Dekiwadia, C.D.; Paul, W.; Shenoy, S.J.; Laloraya, M.; Srinivasula, S.M.; et al. Paradigm of Vanadium pentoxide nanoparticle-induced autophagy and apoptosis in triple-negative breast cancer cells. *bioRxiv* **2019**. [[CrossRef](#)]
56. Ivanković, S.; Musić, S.; Gotić, M.; Ljubesić, N. Cytotoxicity of nanosize V<sub>2</sub>O<sub>5</sub> particles to selected fibroblast and tumor cells. *Toxicol. Vitro* **2006**, *20*, 286–294. [[CrossRef](#)]
57. Litz, J.; Warshamana-Greene, G.S.; Sulanke, G.; Lipson, K.E.; Krystal, G.W. The multi-targeted kinase inhibitor SU5416 inhibits small cell lung cancer growth and angiogenesis, in part by blocking Kit-mediated VEGF expression. *Lung Cancer* **2004**, *46*, 283–291. [[CrossRef](#)] [[PubMed](#)]
58. Kanapathipillai, M. Treating p53 Mutant Aggregation-Associated Cancer. *Cancers* **2018**, *10*, 154. [[CrossRef](#)]
59. Cheung, C.H.A.; Chang, Y.; Lin, T.; Cheng, S.M.; Leung, E. Anti-apoptotic proteins in the autophagic world: An update on functions of XIAP, Survivin, and BRUCE. *J. Biomed. Sci.* **2020**, *27*, 31. [[CrossRef](#)]
60. Kulkarni, A.; Kumar, G.S.; Kaur, J.; Tikoo, K. A comparative study of the toxicological aspects of vanadium pentoxide and vanadium oxide nanoparticles. *Inhal. Toxicol.* **2014**, *26*, 772–788. [[CrossRef](#)]
61. Cohen, M.D.; Sisco, M.; Prophete, C.; Yoshida, K.; Chen, L.; Zelikoff, J.T.; Smee, J.; Holder, A.A.; Stonehuerner, J.; Crans, D.C.; et al. Effects of metal compounds with distinct physicochemical properties on iron homeostasis and antibacterial activity in the lungs: Chromium and vanadium. *Inhal. Toxicol.* **2010**, *22*, 169–178. [[CrossRef](#)] [[PubMed](#)]
62. Al-Qatati, A.; Fontes, F.L.; Barisas, B.G.; Zhang, D.; Roess, D.A.; Crans, D.C. Raft localization of Type I Fcε receptor and degranulation of RBL-2H3 cells exposed to decavanadate, a structural model for V<sub>2</sub>O<sub>5</sub>. *Dalton Trans.* **2013**, *42*, 11912–11920. [[CrossRef](#)]
63. Aureliano, M.; Ohlin, C.A. Decavanadate in vitro and in vivo effects: Facts and opinions. *J. Inorg. Biochem.* **2014**, *137*, 123–130. [[CrossRef](#)]

64. Wu, J.; Hong, Y.; Yang, X. Bis (acetylacetonato)-oxidovanadium (IV) and sodium metavanadate inhibit cell proliferation via ROS-induced sustained MAPK/ERK activation but with elevated AKT activity in human pancreatic cancer AsPC-1 cells. *J. Biol. Inorg. Chem.* **2016**, *21*, 919–929. [[CrossRef](#)] [[PubMed](#)]
65. Fu, Y.; Wang, Q.; Yang, X.G.; Yang, X.D.; Wang, K. Vanadyl bisacetylacetonate induced G1/S cell cycle arrest via high-intensity ERK phosphorylation in HepG2 cells. *J. Biol. Inorg. Chem.* **2008**, *13*, 1001–1009. [[CrossRef](#)] [[PubMed](#)]
66. Rivadeneira, J.; Virgilio, A.L.D.; Barrio, D.A.; Muglia, C.I.; Bruzzone, L.; Etcheverry, S.B. Cytotoxicity of a vanadyl (IV) complex with a multidentate oxygen donor in osteoblast cell lines in culture. *Med. Chem.* **2010**, *6*, 9–23. [[CrossRef](#)]
67. Dankner, M.; Rose, A.A.N.; Rajkumar, S.; Siegel, P.M.; Watson, I.R. Classifying BRAF alterations in cancer: New rational therapeutic strategies for actionable mutations. *Oncogene* **2018**, *37*, 3183–3199. [[CrossRef](#)]
68. Broude, E.V.; Swift, M.E.; Vivo, C.; Chang, B.; Davis, B.M.; Kalurupalle, S.; Blagosklonny, M.V.; Roninson, I.B. p21(Waf1/Cip1/Sdi1) mediates retinoblastoma protein degradation. *Oncogene* **2007**, *26*, 6954–6958. [[CrossRef](#)]
69. Kasthuber, E.R.; Lowe, S.W. Putting p53 in context. *Cell* **2017**, *170*, 1062–1078. [[CrossRef](#)]
70. Padua, M.M.C.; Cadena, S.M.S.C.; Petkowicz, C.L.O.; Martinez, G.R.; Rocha, M.E.M.; Mercê, A.L.R.; Noleto, G.R. Toxicity of native and oxovanadium (IV/V) galactomannan complexes on HepG2 cells is related to impairment of mitochondrial functions. *Carbohydr. Polym.* **2017**, *173*, 665–675. [[CrossRef](#)]
71. Cao, Y.; Ikeda, I. Antioxidant activity and antitumor activity (in vitro) of xyloglucan selenious ester and surfated xyloglucan. *Int. J. Biol. Macromol.* **2009**, *45*, 231–235. [[CrossRef](#)]
72. Kulkarni, A.D.; Joshi, A.A.; Patil, C.L.; Amale, P.D.; Patel, H.M.; Surana, S.J.; Belgamwar, V.S.; Chaudhari, K.S.; Pardeshi, C.V. Xyloglucan: A functional biomacromolecule for drug delivery applications. *Int. J. Biol. Macromol.* **2017**, *104*, 799–812. [[CrossRef](#)]
73. Batista, Â.G.; Ferrari, A.S.; Cunha, D.C.; Silva, J.K.; Cazarin, C.B.B.; Correa, L.C.; Prado, M.A.; Carvalho-Silva, L.B.; Esteves, E.A.; Júnior, M.R.M. Polyphenols, antioxidants, and antimutagenic effects of copaifera langsdorffii fruit. *Food Chem.* **2016**, *197*, 1153–1159. [[CrossRef](#)] [[PubMed](#)]
74. Soares, S.S.; Gutiérrez-Merino, C.; Aureliano, M. Decavanadate induces mitochondrial membrane depolarization and inhibits oxygen consumption. *J. Inorg. Biochem.* **2007**, *101*, 789–796. [[CrossRef](#)] [[PubMed](#)]
75. Banerjee, S.; Prasad, P.; Hussain, A.; Khan, I.; Kondaiah, P.; Chakravarty, A.R. Remarkable photocytotoxicity of curcumin in HeLa cells in visible light and arresting its degradation on oxovanadium (IV) complex formation. *Chem. Commun.* **2012**, *48*, 7702–7704. [[CrossRef](#)] [[PubMed](#)]
76. Banerjee, S.; Hussain, A.; Prasad, P.; Khan, I.; Banik, B.; Kondaiah, P.; Chakravarty, A.R. Photocytotoxic oxidovanadium (IV) complexes of polypyridyl ligands showing DNA-cleavage activity in near-IR light. *Eur. J. Inorg. Chem.* **2012**, *2012*, 3899–3908. [[CrossRef](#)]
77. Sasmal, P.K.; Patra, A.K.; Nethaji, M.; Chakravarty, A.R. DNA cleavage by new oxovanadium (IV) complexes of N-salicylidene alpha-amino acids and phenanthroline bases in the photodynamic therapy window. *Inorg. Chem.* **2007**, *46*, 11112–11121. [[CrossRef](#)] [[PubMed](#)]
78. Kawashima, T.; Ohkubo, K.; Fukuzumi, S. Photoinduced DNA cleavage by formation of ROS from oxygen with a neurotransmitter and aromatic amino acids. *Org. Biomol. Chem.* **2010**, *8*, 994–996. [[CrossRef](#)]
79. Siveen, K.S.; Kuttan, G. Inhibition of B16F-10 Melanoma—induced lung metastasis in C57BL/6 Mice by aerva lanata via induction of apoptosis. *Integr. Cancer Ther.* **2013**, *12*, 81–92. [[CrossRef](#)]
80. Pattanayak, P.; Pratihari, J.L.; Patra, D.; Mitra, S.; Bhattacharyya, A.; Lee, H.M.; Chattopadhyay, S. Synthesis, structure and reactivity of azosalophen complexes of vanadium (IV): Studies on cytotoxic properties. *Dalton Trans.* **2009**, *31*, 6220–6230. [[CrossRef](#)]
81. Sheth, S.; Mukherjee, D.; Rybak, L.P.; Ramkumar, V. Mechanisms of cisplatin-induced ototoxicity and otoprotection. *Front. Cell. Neurosci.* **2017**, *11*, 338. [[CrossRef](#)] [[PubMed](#)]
82. Bahrami, B.; Mohammadnia-Afrouzi, M.; Bakhshaei, P.; Yazdani, Y.; Ghalamfarsa, G.; Yousefi, M.; Sadreddini, S.; Jadidi-Niaragh, F.; Hojjat-Farsangi, M. Folate-conjugated nanoparticles as a potent therapeutic approach in targeted cancer therapy. *Tumour Biol.* **2015**, *36*, 5727–5742. [[CrossRef](#)] [[PubMed](#)]
83. Bai, L.; Gao, C.; Liu, Q.; Yu, C.; Zhang, Z.; Cai, L.; Yang, B.; Qian, Y.; Yang, J.; Liao, X. Research progress in modern structure of platinum complexes. *Eur. J. Med. Chem.* **2017**, *140*, 349–382. [[CrossRef](#)] [[PubMed](#)]
84. Ursic, K.; Kos, S.; Kamensek, U.; Cemazar, M.; Scancar, J.; Bucek, S.; Kranjc, S.; Staresinic, B.; Sersa, G. Comparable effectiveness and immunomodulatory actions of oxaliplatin and cisplatin in electrochemotherapy of murine melanoma. *Bioelectrochemistry* **2018**, *119*, 161–171. [[CrossRef](#)] [[PubMed](#)]
85. Doherty, A.T. The in vitro micronucleus assay. *Methods Mol. Biol.* **2012**, *817*, 121–141. [[CrossRef](#)] [[PubMed](#)]
86. Gumerova, N.I.; Rompel, A. Interweaving disciplines to advance chemistry: Applying polyoxometalates in biology. *Inorg. Chem.* **2021**, *60*, 6109–6114. [[CrossRef](#)]